

Disentangling Pivotality and Campaign Mobilization in U.S. Presidential Elections

Luke Miller
Georgetown University

June 6, 2025

Abstract

Voter turnout is systematically higher in competitive elections, but existing models struggle to disentangle the mechanisms behind this pattern. This paper develops and estimates a structural model of turnout that integrates two key forces: pivotal voting incentives, which increase with the closeness of the race, and campaign-driven mobilization, which shifts the utility differential in favor of a candidate’s supporters. In the model, presidential candidates strategically allocate campaign effort across states to maximize their probability of winning the Electoral College, anticipating that voters will respond both to direct mobilization and to the endogenously determined competitiveness of the contest. The model is estimated by maximum likelihood using county-level data from the 2008–2020 U.S. presidential elections. Counterfactual simulations reveal that pivotality explains roughly 25% of the turnout gap between battleground and non-battleground states, while campaign mobilization accounts for the remaining 75%. The model also reconciles the puzzle of modest experimental treatment effects with large-scale campaign spending: although marginal returns are low, the average cost per vote remains modest, making such investments rational from the campaign’s perspective.

1 Introduction

Voter turnout is consistently higher in competitive elections than in those with a clear expected winner. Two mechanisms help explain this pattern. First, as the expected margin of victory narrows, the probability an individual vote is pivotal to changing the outcome of the election increases, raising the instrumental value of voting (Downs 1957; Palfrey and Rosenthal 1983; Castanheira 2003; Myatt 2012). Second, campaigns concentrate their efforts in tightly contested races, mobilizing voters through outreach and persuasion that increase the perceived benefits or reduce the costs of participation (Gerber and Green 2000; Shachar and Nalebuff 1999). These channels frequently operate in tandem: competitive elections tend to attract greater campaign resources, and increased mobilization

can in turn alter the competitive landscape. This co-movement complicates empirical analysis, as it becomes difficult to isolate the distinct contributions of pivotal incentives and direct mobilization.

Recent presidential elections illustrate this dynamic. As Table 1 shows, in each cycle from 2008 to 2020, a small set of states attracted the vast majority of campaign activity. Specifically, the ten states with the highest combined Democratic and Republican television advertising accounted for over 85% of total television advertising spending in each election. These “battleground” states also exhibited much tighter electoral margins, averaging just 2.5 percentage points compared to 10.2 in non-battleground states. They also had substantially higher voter turnout, averaging 62.6% versus 56.5%.

Table 1: Battleground vs. Non-Battleground States

	Battleground	Non-Battleground
Avg. Margin (%)	2.5	10.2
TV Ad Share (%)	85	15
Turnout Rate (%)	62.6	56.5

Note: Battleground states are defined as the top 10 states by combined Democratic and Republican television advertising expenditures in each presidential election year (2008, 2012, 2016, 2020). Turnout is measured as the share of eligible voters who cast a ballot.

A further puzzle complicates the interpretation of these patterns. Despite the scale, sophistication, and strategic targeting of modern campaigns, many reduced-form studies and field experiments report only modest or statistically insignificant turnout effects from campaign spending (Ashworth, Clinton, et al. 2007; Spenkuch and Toniatti 2018; Aggarwal et al. 2023). This disconnect raises fundamental questions about how and for whom mobilization efforts matter, and whether their effects are fully captured by standard empirical approaches.

Together, these empirical patterns point to a gap in existing theory: even as both mechanisms appear important, formal models typically treat them in isolation. This is especially true of structurally estimated models, which endogenize either voter behavior or candidate strategy, but rarely both. Models that focus on pivotal voting abstract away from campaign effort (e.g., Coate and Conlin (2004), Coate, Conlin, and Moro (2008), and Kawai, Toyama, and Watanabe (2021)), while mobilization models (e.g. Strömberg (2008) and Shachar and Nalebuff (1999)) overlook how strategic spending reshapes electoral competitiveness and shut down endogenous turnout responses.

This separation is especially problematic because effort and competitiveness may be jointly determined in equilibrium. For example, when a trailing candidate increases effort, the expected margin of victory may narrow, increasing the perceived competitiveness of the race and potentially amplifying turnout. Conversely, if a frontrunner ramps up spending, the expected margin may widen, dampening the efficacy of that effort by reducing the competitiveness of the

race.

To address this gap, this paper develops and estimates a novel structural model of voter turnout that fully integrates both competitive voting incentives and campaign mobilization within a unified equilibrium framework. Presidential candidates strategically allocate finite campaign budgets across states to maximize their probability of winning the national election. Crucially, they do so anticipating that voters will respond not only to direct mobilization stemming from this spending but also to the endogenously determined competitiveness of the contest. Voters, in turn, decide whether to turn out after observing campaign effort, considering the expected utility differential between candidates, the competitiveness of the election, and their cost of voting.

The model is estimated by maximum likelihood using county-level data from the 2008–2020 U.S. presidential elections. Counterfactual exercises allow me to disentangle the effects of each channel by separately (i) removing campaign effort and (ii) equalizing electoral competitiveness across states. This approach enables a decomposition of observed turnout differences into their pivotal and mobilization components. The model also yields estimates of the marginal and average cost of mobilizing votes, offering insight into the efficiency of campaign spending. Although marginal returns to campaign spending are low at observed levels, the model shows that the average cost of generating a vote remains modest. This distinction helps reconcile why campaigns invest heavily in competitive states, even though reduced-form studies often find small or insignificant marginal effects.

Main findings.

1. Differences in electoral competitiveness account for roughly 25% of the turnout gap between battleground and non-battleground states, with the remaining 75% attributable to direct mobilization efforts by campaigns.
2. The model reconciles the puzzle of small experimental spending effects with large campaign budgets: while the average cost of generating an additional vote is estimated to be \$30–\$40, the marginal cost at current observed spending levels exceeds \$500.

The paper proceeds as follows. Section 2 reviews the relevant literature on voting behavior and campaign mobilization. Section 3 presents the model, detailing voter and candidate behavior across the three stages of the electoral process. Section ?? describes the estimation strategy and data sources. Section 6 presents the main results, including parameter estimates and counterfactual decompositions. Section 7 discusses the implications of the findings for understanding voter turnout and campaign strategy, Section 8 concludes with a discussion of the implications for understanding voter turnout and campaign strategy.

2 Literature

The canonical rational-choice model posits that individuals vote when

$$p \cdot \Delta u - c + d > 0,$$

where p is the probability of casting a decisive vote, Δu the utility differential between candidates, c the cost of voting, and d the expressive benefit of participation (Downs 1957; Riker and Ordeshook 1968). Although pivotality plays a central role in this framework, its influence on turnout becomes negligible in realistically sized elections.

For example, consider Wyoming, the smallest U.S. state by voting-eligible population between 2008 and 2020, with roughly 400,000 eligible voters. Assume each individual votes with 50% probability, and the expected margin between the two candidates is only 0.5 percentage points. Under these assumptions, the probability of casting a decisive vote is on the order of $10^{-6}\%$. In an average-sized state with 5 million eligible voters, the corresponding probability falls to just $10^{-54}\%$.¹ Thus, even in seemingly close contests, the odds of a single vote determining the outcome are vanishingly small in large electorates.

Theoretical refinements to the standard model attempt to rationalize voting in such settings. Palfrey and Rosenthal (1983) extend the Downsian framework to a game-theoretic setting in which voters adopt mixed strategies. Even in this richer formulation, however, the probability of casting a decisive vote remains exceedingly small. Castanheira (2003) argues voters may care not only about whether their preferred candidate wins, but also about the margin of victory. A larger margin strengthens the winning candidate's perceived mandate, enabling the implementation of more preferred policies. This generates incentives to vote even when the outcome is not in doubt. Myatt (2012) shows that introducing uncertainty about the aggregate preferences of the electorate, in addition to altruistic motivations, can increase a voter's expected probability of casting a decisive vote to a non-negligible level even in large elections.

A complementary strand of the literature attributes higher turnout in competitive elections to strategic campaign activity. Candidates can reduce voting costs or heighten the perceived stakes of the contest, raising participation rates in close races (Shachar and Nalebuff 1999). Herrera, Levine, and Martinelli (2008) extends this idea by modeling both campaign effort and policy positioning as strategic choices, reflecting the dual levers available to candidates.

¹These estimates are based on the analytical approximation in Myerson (2000). In a Poisson voting game, the pivotal probability is given by

$$\pi(n, \tau_A, \tau_B) = \frac{\exp[n(2\sqrt{\tau_A\tau_B} - \tau_A - \tau_B)]}{4\sqrt{\pi n\sqrt{\tau_A\tau_B}}} \cdot \left(\frac{\sqrt{\tau_A} + \sqrt{\tau_B}}{\sqrt{\tau_A}} \right),$$

where n is the expected number of voters and τ_A, τ_B are the turnout probabilities for candidates A and B. In a fixed- n setting with homogeneous turnout, the probability decays even more sharply:

$$\pi_{\text{fixed}}(n, \mu) \approx \exp(n \log(1 + \mu)), \quad \text{with } \mu = \frac{\log \pi}{n}.$$

Closest to the approach in this paper, Strömberg (2008) estimates a structural model in which presidential candidates allocate resources across states to maximize their electoral chances. However, these models treat turnout as fixed, abstracting from how voters may respond to campaign intensity or to the overall competitiveness of the election. As a result, they are unable to distinguish whether higher turnout in competitive states arises from increased pivotality, greater campaign effort, or the interaction between the two.

Empirically, closer contests are consistently associated with higher participation (Geys 2006). However, reduced-form and experimental evidence offers mixed findings. Gerber (2004) and Nickerson (2006) report large turnout effects from door-to-door canvassing and high-quality phone outreach, respectively. By contrast, Spenkuch and Toniatti (2018) find negligible effects from television advertising, while Aggarwal et al. (2023) document only modest average effects of digital ads, though with some evidence of heterogeneity in treatment responses. Enos and Fowler (2018) compare turnout across battleground and non-battleground states, concluding that campaign spending increases turnout by 8–10 percentage points. Yet their identification strategy assumes competitiveness is exogenous to turnout—an assumption this paper relaxes.

Other work focuses more directly on the causal effect of competitiveness itself. Both Fraga, Moskowitz, and Schneer (2022) and Ainsworth, Munoz, and Gomez (2022) exploit redistricting-induced changes in electoral competitiveness. Yet their findings diverge: Fraga, Moskowitz, and Schneer (2022) find limited effects, while Ainsworth, Munoz, and Gomez (2022) show that competitiveness increases turnout. Complementing these U.S.-based studies, Bursztyrn et al. (2024) use polling shocks in Swiss referenda to show that increases in perceived electoral closeness significantly boost participation, reinforcing the view that competitiveness shapes turnout behavior through more than just campaign spending.

Despite evidence showing that both pivotal incentives and campaign mobilization play a role in explaining turnout, all structurally estimated models of turnout (to the best of my knowledge) treat either voter or candidate behavior as fixed. Candidate-focused models such as Strömberg (2008) and Shachar and Nalebuff (1999) endogenize campaign effort but assume full turnout. Voter-centric models (e.g., Coate and Conlin 2004; Coate, Conlin, and Moro 2008; Kawai, Toyama, and Watanabe 2021) allow turnout to respond to preferences or voting costs, but treat campaign behavior as exogenous. For instance, Kawai, Toyama, and Watanabe (2021) develop a costly-voting model in which turnout depends on preference intensity, the cost of voting, and a reduced-form measure they term *perceived voting efficacy*. This parameter captures a voter’s expected utility gain from voting given beliefs about the aggregate vote. However, it is introduced as a reduced-form object rather than being derived from an underlying equilibrium model, and it does not incorporate strategic responses to or by campaign activity. In contrast, in my framework perceived efficacy is an equilibrium object—determined by the endogenous level of turnout, which reflects both voters’ underlying preferences and the effects of campaign effort on participation costs and incentives.

A parallel line of research emphasizes how administrative frictions shape voter participation by altering either the cost of voting or the salience of the election. Several studies find that expanding access through vote-by-mail modestly increases turnout, particularly in lower-salience elections (Gerber, Huber, and S. J. Hill 2013; Thompson et al. 2020; Bonica et al. 2021). Cantoni (2020) show that increasing the distance to a polling place by one standard deviation reduces turnout by 2–5 percentage points, highlighting how even minor logistical burdens can discourage participation. Using a broader sample of states and more granular geographic data, Bagwe, Margitic, and Stashko (2022) find similar patterns, with larger effects in urban areas where potential voters need to rely more on public transportation.

Evidence on voter ID laws is more mixed and appears to depend on context. Cantoni and Pons (2021) find little evidence that stricter ID requirements affect turnout at the aggregate level. By contrast, Harden and Campos (2023) argue that these laws may actually increase participation in some settings by heightening the perceived stakes of the election, particularly among partisan or highly engaged voters.

3 Model of Turnout and Campaign Strategy

Two candidates, D (Democrat) and R (Republican), compete in a U.S.-style presidential election decided by the Electoral College. To win the election, a candidate must accumulate 270 electoral votes. Each state $s \in \mathcal{S}$ gives its assigned electoral votes l_s to a candidate using a first-past-the-post election.

Candidates have a fixed, exogenous amount of effort, denoted E_D and E_R . They choose how to allocate their effort across states in order to maximize their probability of winning the election. Voters care only about the election outcome of their respective state. Each state s is partitioned into counties indexed by $j_s \in \mathcal{J}_s$, where $\sum_{j_s \in \mathcal{J}_s} w_{j_s} = 1$ and w_{j_s} denotes the county’s share of the state’s voting-eligible population.

There are three stages of the model:

1. **Pre-campaign stage:** Individuals hold initial preferences over the two parties.
2. **Campaign.** Observing state-level preference distributions, candidates allocate effort $\{e_{s,D}, e_{s,R}\}_{s \in \mathcal{S}}$ subject to $\sum_s e_{s,D} \leq E_D$ and $\sum_s e_{s,R} \leq E_R$. Effort shifts voters’ utility differentials.
3. **Election.** Voters decide whether to turn out and who to vote for, evaluating the utility differential between the two candidates, the cost of voting, and the competitiveness of the election.

I will first discuss voter behavior in stages 1 and 3, then return to stage 2 to discuss campaign strategy.

3.1 Stage 1: Pre-Campaign Stage

In the pre-campaign stage, individuals hold pre-existing preferences for the two candidates. Let $\Delta\tilde{u}_{i,j_s}$ denote the baseline utility differential between candidate R and candidate D for individual i in county j_s of state s . A positive value indicates a preference for R , and a negative value indicates a preference for D .

The differential is given by:

$$\Delta\tilde{u}_{i,j_s} = \mu_{j_s} - \eta_{j_s} - \delta_s - \epsilon_{i,j_s},$$

where μ_{j_s} captures the average partisan lean of county j_s , while the remaining terms introduce heterogeneity across counties, states, and individuals. Specifically, $\eta_{j_s} \sim \mathcal{N}(0, \sigma_\eta^2)$ is a county-level deviation from the baseline; $\delta_s \sim \mathcal{N}(0, \sigma_\delta^2)$ is a common statewide shock; and $\epsilon_{i,j_s} \sim \mathcal{N}(0, \sigma_\epsilon^2)$ reflects idiosyncratic preference noise at the individual level. The state and county-level shocks capture systematic factors that shift attitudes toward candidate R uniformly across the state or county, such as gubernatorial popularity, salient statewide policy, or national partisan narratives disproportionately affecting a given state or county.

All shocks are mean-zero and independently distributed. Positive realizations reduce support for R , shifting voters toward D . Because each component enters symmetrically and additively, the county fixed effect μ_{j_s} represents the expected pre-campaign utility advantage of candidate R in county j_s .

3.2 Stage 3: Election Stage

After candidates exert effort during the campaign, individuals form updated utility differentials that determine their voting behavior. Let $e_{s,D}$ and $e_{s,R}$ denote the per-capita spending (or effort) of candidates D and R in state s , respectively.

Following the campaign, the utility differential for individual i in county j_s in state s is given by:

$$\Delta u_{i,j_s} = \begin{cases} \min(-u(e_{s,D}) + \mu_{j_s} - \eta_{j_s} - \delta_s + \eta_{j_s}^p - \epsilon_{i,j_s}, 0), & \text{if } \Delta\tilde{u}_{i,j_s} < 0, \\ \max(u(e_{s,R}) + \mu_{j_s} - \eta_{j_s} - \delta_s - \eta_{j_s}^p - \epsilon_{i,j_s}, 0), & \text{if } \Delta\tilde{u}_{i,j_s} \geq 0. \end{cases}$$

The function $u(\cdot)$ maps candidate effort into utility gains and is assumed to be increasing and concave. Effort affects only those individuals who were initially predisposed to support a given candidate; that is, candidate D (respectively, R) affects only those with $\Delta\tilde{u}_{i,j_s} < 0$ (respectively, $\Delta\tilde{u}_{i,j_s} \geq 0$).²

After the campaign, individuals receive a new county-level shock $\eta_{j_s}^p \sim \mathcal{N}(0, \sigma_\eta^2)$ that perturbs their latent utility differential.³ Positive realizations of $\eta_{j_s}^p$ moderate voter preferences, moving utility differentials closer to zero, while

²As a robustness check, I estimate an alternative specification allowing cross-party persuasion. The model fit is worse, suggesting that the mobilization-only assumption better matches the data.

³I assume that $\eta_{j,s}$ and $\eta_{j_s}^p$ are independent, though drawn from the same distribution.

negative realizations intensify partisan attachments by pushing utility differentials further from zero.

To preserve internal consistency (that is, to prevent post-campaign shocks from reversing an individual's baseline partisan alignment) I explicitly truncate $\Delta u_{i,j_s}$, ensuring it remains non-positive for voters initially aligned with D and non-negative for those aligned with R . Without this truncation, sufficiently large realizations of $\eta_{j_s}^p$ could flip a voter's utility differential across zero, violating the model's assumption of fixed partisan identity.

Voters also face a cost of voting, c_{j_s} , that varies by county. A voter will turn out only if the expected benefit of voting exceeds this cost. The expected benefit depends on perceived voting efficacy⁴ at the state level, denoted $p(\sigma_{s,D}, \sigma_{s,R})$, where $\sigma_{s,D}$ and $\sigma_{s,R}$ are the aggregate turnout rates of D and R in state s .

I assume that $p(\sigma_{s,D}, \sigma_{s,R})$ is increasing in electoral competitiveness, reaching its maximum when the election is a tie. The exact functional form is described in the estimation section.

An individual in county j_s votes for D if $\Delta \tilde{u}_{i,j_s} < 0$ and:

$$p(\sigma_{s,D}, \sigma_{s,R}) \cdot |\Delta u_{i,j_s}| > c_{j_s},$$

and votes for R if $\Delta \tilde{u}_{i,j_s} \geq 0$ and:

$$p(\sigma_{s,D}, \sigma_{s,R}) \cdot \Delta u_{i,j_s} > c_{j_s}.$$

Let $H(\cdot)$ denote the cumulative distribution function of the individual-specific shock ϵ_{i,j_s} , which is assumed to follow a normal distribution with mean zero and variance σ_ϵ^2 . Given the large number of voters in each county, individual turnout decisions can be aggregated to obtain county-level voting shares. The fraction of eligible voters in county j_s who vote for candidate D is given by:

$$\sigma_{j_s,D} = H\left(u(e_{s,D}) - \mu_{j_s} - \frac{c_{j_s}}{p(\sigma_{s,D}, \sigma_{s,R})} + \eta_{j_s} + \delta_s - \eta_{j_s}^p\right), \quad (1)$$

and the fraction voting for R is:

$$\sigma_{j_s,R} = H\left(u(e_{s,R}) + \mu_{j_s} - \frac{c_{j_s}}{p(\sigma_{s,D}, \sigma_{s,R})} - \eta_{j_s} - \delta_s - \eta_{j_s}^p\right). \quad (2)$$

These expressions for turnout shares are derived by determining the threshold for the idiosyncratic shock ϵ_{i,j_s} under which a voter turns out.⁵

⁴The term *perceived voting efficacy* follows Kawai, Toyama, and Watanabe (2021), who introduce it as a reduced-form object capturing how voters internalize their influence on the election outcome, in a costly voting model. In contrast, I embed efficacy as an endogenous function of state-level turnout rates, allowing it to vary structurally with electoral competitiveness.

⁵For a D-leaning voter, the turnout condition is $p(\sigma_{s,D}, \sigma_{s,R}) \cdot |\Delta u_{i,j_s}| > c_{j_s}$. Since

The fraction of eligible voters in county j_s who abstain is denoted by $\sigma_{j_s,A}$. By construction,

$$\sigma_{j_s,D} + \sigma_{j_s,R} + \sigma_{j_s,A} = 1.$$

These county-level voting shares, including abstention, depend endogenously on the state-level aggregates $\sigma_{s,D}$ and $\sigma_{s,R}$, reflecting the equilibrium relationship between individual turnout decisions and perceived voting efficacy.

3.3 Stage 2: Campaign Stage

3.3.1 Candidates' Objective Function

Each candidate allocates a fixed, exogenously given amount of resources to maximize the probability of winning the election. Let E_D and E_R denote the total campaign resources available to candidates D and R , respectively.

To reflect the reality of U.S. presidential elections and to reduce computational complexity, I assume that certain states are safe for each party and receive zero campaign effort. Let BG denote the set of battleground states where outcomes are uncertain and candidates allocate positive effort. The safe states contribute their electoral votes automatically to the respective candidate's total. Let EV_D and EV_R denote the number of electoral votes secured by candidates D and R from safe states, respectively.⁶

Candidates concentrate their campaign effort in battleground states and choose allocations to maximize their probability of winning the Electoral College. In making these decisions, they account for how voter turnout responds to campaign effort and perceived electoral competitiveness. Specifically, they consider the distribution of partisan preferences across counties, the cost of voting, and how these factors jointly shape turnout through the perceived efficacy function $p(\sigma_{s,D}, \sigma_{s,R})$, which increases with the closeness of the contest.

While candidates do not observe the realization of local preference shocks $\eta_{j_s}, \delta_s, \eta_{j_s}^p$, they are assumed to know their distribution. This allows them to

$\Delta u_{i,j_s} = -u(e_{s,D}) + \mu_{j_s} - \eta_{j_s} - \delta_s + \eta_{j_s}^p - \epsilon_{i,j_s}$, its absolute value is

$$|\Delta u_{i,j_s}| = u(e_{s,D}) - \mu_{j_s} + \eta_{j_s} + \delta_s - \eta_{j_s}^p + \epsilon_{i,j_s}.$$

Substituting and solving for ϵ_{i,j_s} gives

$$\epsilon_{i,j_s} > \frac{c_{j_s}}{p(\sigma_{s,D}, \sigma_{s,R})} - u(e_{s,D}) + \mu_{j_s} - \eta_{j_s} - \delta_s + \eta_{j_s}^p \equiv K.$$

Since $\epsilon_{i,j_s} \sim \mathcal{N}(0, \sigma_\epsilon^2)$, the turnout probability is $1 - H(K) = H(-K)$. The argument of $H(\cdot)$ in equation (1) is precisely $-K$:

$$-K = u(e_{s,D}) - \mu_{j_s} - \frac{c_{j_s}}{p(\sigma_{s,D}, \sigma_{s,R})} + \eta_{j_s} + \delta_s - \eta_{j_s}^p.$$

A similar derivation applies for R-leaning voters.

⁶For empirical support for the battleground / non-battleground state distinction, see, e.g., <https://fairvote.org/report/2008-s-shrinking-battleground-and-its-stark-impact-on-campaign-activity/> and author calculations based on data from the Wesleyan Media Project, which show that over 85% of television advertising and 90% of campaign visits during the 2008–2020 presidential elections occurred in just 10 states on average.

compute expected turnout rates as a function of both their own and their opponent's campaign effort. Using these expectations, candidates allocate resources across states to maximize the probability that their total electoral vote count meets or exceeds the 270-vote threshold required to win.

Candidate D 's problem can be written as:

$$\max_{\{e_{s,D}\}_{s \in BG}} \Pr \left(EV_D + \sum_{s \in BG} D_s l_s \geq 270 \right) \quad \text{subject to} \quad \sum_{s \in BG} n_s \cdot e_{s,D} \leq E_D,$$

where n_s is the voting age population in state s and l_s denotes the number of electoral votes in state s , and $D_s = 1$ if candidate D wins state s , and zero otherwise.⁷

The probability candidate D wins state s depends on the state-level aggregate vote shares, and is denoted:

$$p_s(e_{s,D}, e_{s,R}) \equiv \Pr(\sigma_{s,D}(e_{s,D}, e_{s,R}) > \sigma_{s,R}(e_{s,D}, e_{s,R})),$$

where $\sigma_{s,D}(e_{s,D}, e_{s,R})$ and $\sigma_{s,R}(e_{s,D}, e_{s,R})$ denote the shares of the total eligible voting population turning out for D and R in state s , respectively, as functions of the candidates' efforts.

Since state-level outcomes are conditionally independent given efforts, and because the number of battleground states is sufficiently large, I approximate the distribution of the total electoral votes obtained by candidate D using the Central Limit Theorem.⁸ Specifically, $\sum_{s \in BG} D_s l_s$ is approximated by a normal distribution with mean and variance:

$$\sum_{s \in BG} D_s l_s \sim \mathcal{N} \left(\sum_{s \in BG} p_s(e_{s,D}, e_{s,R}) l_s, \sum_{s \in BG} p_s(e_{s,D}, e_{s,R}) (1 - p_s(e_{s,D}, e_{s,R})) l_s^2 \right).$$

Under this approximation, candidate D 's objective function becomes:

$$\begin{aligned} \max_{\{e_{s,D}\}_{s \in BG}} \quad & \Phi \left(\frac{\sum_{s \in BG} p_s(e_{s,D}, e_{s,R}) \cdot l_s - (270 - EV_D)}{\sqrt{\sum_{s \in BG} p_s(e_{s,D}, e_{s,R}) [1 - p_s(e_{s,D}, e_{s,R})] l_s^2}} \right) \\ \text{subject to} \quad & \sum_{s \in BG} n_s \cdot e_{s,D} \leq E_D \end{aligned} \quad (3)$$

where $\Phi(\cdot)$ denotes the cumulative distribution function of the standard normal distribution.

Similarly, candidate R 's objective function is:

⁷I abstract from states like Maine and Nebraska, which allocate electoral votes by congressional district.

⁸Strömberg (2008) follows a similar approach in approximating expected electoral vote counts under conditional independence across states.

$$\begin{aligned}
& \max_{\{e_{s,R}\}_{s \in BG}} \Phi \left(\frac{\sum_{s \in BG} [1 - p_s(e_{s,D}, e_{s,R})] \cdot l_s - (270 - EV_R)}{\sqrt{\sum_{s \in BG} p_s(e_{s,D}, e_{s,R}) [1 - p_s(e_{s,D}, e_{s,R})] l_s^2}} \right) \\
& \text{subject to } \sum_{s \in BG} n_s \cdot e_{s,R} \leq E_R
\end{aligned} \tag{4}$$

3.3.2 Calculating the Probability of Winning a State

The probability a candidate wins a state depends on individual-level voting decisions. For candidate D , the probability of winning state s is:

$$\begin{aligned}
& \Pr \left(\sigma_{s,D}(e_{s,D}, e_{s,R}) > \sigma_{s,R}(e_{s,D}, e_{s,R}) \right) \\
& = \Pr \left(\sum_{j_s} w_{j_s} \sigma_{j_s,D} - \sum_{j_s} w_{j_s} \sigma_{j_s,R} > 0 \right), \tag{5}
\end{aligned}$$

where, following the structure from Section 3.2:

$$\begin{aligned}
\sigma_{j_s,D} &= H \left(u(e_{s,D}) - \mu_{j_s} - \frac{c_{j_s}}{p(\sigma_{s,D}, \sigma_{s,R})} + \eta_{j_s} + \delta_s - \eta_{j_s}^p \right), \\
\sigma_{j_s,R} &= H \left(u(e_{s,R}) + \mu_{j_s} - \frac{c_{j_s}}{p(\sigma_{s,D}, \sigma_{s,R})} - \eta_{j_s} - \delta_s - \eta_{j_s}^p \right).
\end{aligned}$$

There are two main challenges in directly solving for the probability in (5). First, the probability depends on three random components: the county-specific shocks η_{j_s} and $\eta_{j_s}^p$, and the state-specific shock δ_s . Second, the county-level turnout rates $\sigma_{j_s,D}$ and $\sigma_{j_s,R}$ depend endogenously on the statewide aggregates $\sigma_{s,D}$ and $\sigma_{s,R}$.

To simplify, I approximate the probability of winning a state by assuming that candidates treat county-level shocks η_{j_s} and $\eta_{j_s}^p$ as negligible relative to the state-level shock δ_s . This is justified when the variance of county-level shocks is small compared to the variance of the state-level shock, and there are many counties in the state, as shown in Appendix ??.

Under this approximation, define the adjusted county-level turnout shares as:

$$\begin{aligned}
\tilde{\sigma}_{j_s,D} &= H \left(u(e_{s,D}) - \mu_{j_s} - \frac{c_{j_s}}{p(\tilde{\sigma}_{s,D}, \tilde{\sigma}_{s,R})} + \delta_s \right), \\
\tilde{\sigma}_{j_s,R} &= H \left(u(e_{s,R}) + \mu_{j_s} - \frac{c_{j_s}}{p(\tilde{\sigma}_{s,D}, \tilde{\sigma}_{s,R})} - \delta_s \right),
\end{aligned}$$

The probability that the Democratic candidate wins state s is then approximated by:

$$p_s(e_{s,D}, e_{s,R}) \approx \Pr \left(\sum_{j_s} w_{j_s} \tilde{\sigma}_{j_s,D} - \sum_{j_s} w_{j_s} \tilde{\sigma}_{j_s,R} > 0 \right).$$

Let $\hat{\delta}_s$ be the threshold value of δ_s at which the weighted support for D and R exactly balance:

$$\begin{aligned} \sum_{j_s} w_{j_s} H \left(u(e_{s,D}) - \mu_{j_s} - \frac{c_{j_s}}{p(\tilde{\sigma}_{s,D}, \tilde{\sigma}_{s,R})} + \hat{\delta}_s \right) = \\ \sum_{j_s} w_{j_s} H \left(u(e_{s,R}) + \mu_{j_s} - \frac{c_{j_s}}{p(\tilde{\sigma}_{s,D}, \tilde{\sigma}_{s,R})} - \hat{\delta}_s \right) \end{aligned} \quad (6)$$

When $\delta_s > \hat{\delta}_s$, candidate D wins the state; otherwise, candidate R wins. Thus, conditional on effort profiles $(e_{s,D}, e_{s,R})$, the winning probability is:

$$p_s(e_{s,D}, e_{s,R}) \approx 1 - F(\hat{\delta}_s) \equiv \tilde{p}_s(e_{s,D}, e_{s,R}), \quad (7)$$

where $F(\cdot)$ denotes the cumulative distribution function of the state-level shock δ_s .

Substituting $\tilde{p}_s(e_{s,D}, e_{s,R})$ for $p_s(e_{s,D}, e_{s,R})$ yields the following objective functions:

$$\begin{aligned} \max_{\{e_{s,D}\}_{s \in BG}} \Phi \left(\frac{\sum_{s \in BG} \tilde{p}_s(e_{s,D}, e_{s,R}) l_s - (270 - EV_D)}{\sqrt{\sum_{s \in BG} \tilde{p}_s(e_{s,D}, e_{s,R}) (1 - \tilde{p}_s(e_{s,D}, e_{s,R})) l_s^2}} \right) \\ \text{subject to } \sum_{s \in BG} n_s \cdot e_{s,D} \leq E_D, \end{aligned} \quad (8)$$

$$\begin{aligned} \max_{\{e_{s,R}\}_{s \in BG}} \Phi \left(\frac{\sum_{s \in BG} (1 - \tilde{p}_s(e_{s,D}, e_{s,R})) l_s - (270 - EV_R)}{\sqrt{\sum_{s \in BG} \tilde{p}_s(e_{s,D}, e_{s,R}) (1 - \tilde{p}_s(e_{s,D}, e_{s,R})) l_s^2}} \right) \\ \text{subject to } \sum_{s \in BG} n_s \cdot e_{s,R} \leq E_R. \end{aligned} \quad (9)$$

3.3.3 Equilibrium Strategies

Given the approximated win probabilities $\tilde{p}_s(e_{s,D}, e_{s,R})$, I solve for a pure-strategy Nash equilibrium in campaign effort. Each candidate $C \in \{D, R\}$ selects an effort allocation $\{e_{s,C}^*\}_{s \in BG}$ to maximize their probability of winning the Electoral College, taking the opponent's allocation as given (see equations (8) and (9)).

The equilibrium conditions correspond to the Karush–Kuhn–Tucker (KKT) system for each candidate's constrained optimization problem, subject to $\sum_{s \in BG} n_s \cdot e_{s,C} \leq E_C$. I solve this system jointly for both candidates using an iterative root-finding algorithm, updating effort vectors until convergence to a fixed point where neither candidate has an incentive to deviate.

4 Estimation

4.1 Estimation Framework

I estimate a vector of structural parameters

$$\Theta = (\beta_\mu, \beta_c, \alpha_1, \alpha_2, \theta, \sigma_\eta, \sigma_\delta)$$

that governs county heterogeneity in partisanship and voting costs, the curvature of the pivotality function, the responsiveness of aggregate turnout to campaign effort, and the variance of the county- and state-level shocks. The variances are normalized to the idiosyncratic Normal shocks (ϵ_{js}), which is assumed to have unit variance.

The empirical strategy exploits county-level vote-share data for U.S. presidential elections from 2008 through 2020, matched to covariates that proxy for baseline partisanship (X_{js}^μ) and voting costs (X_{js}^c). Conditional on these observed characteristics, county turnout shares ($\sigma_{js,D}, \sigma_{js,R}$) aggregate to the state level shares ($\sigma_{s,D}, \sigma_{s,R}$), enter the perceived pivotality term $p(\cdot)$, and interact with endogenous campaign effort in the equilibrium described earlier.

Formally, I maximize the log-likelihood

$$\hat{\Theta} = \arg \max_{\Theta} \sum_{t=2008}^{2020} \sum_{s \in \mathcal{S}} \sum_{j \in \mathcal{J}_s} \log f(\sigma_{jst,D}, \sigma_{jst,R} \mid \Theta; X_{jst}^\mu, X_{jst}^c).$$

where $f(\cdot)$ is the joint density of observed county-level turnout shares, derived under the model's equilibrium. This density embeds three key elements: (i) the mapping from covariates to latent utilities and costs of voting, (ii) the endogenous best-response campaign efforts across states, and (iii) the distributional assumptions on unobserved county- and state-level shocks ($\eta_{js}, \eta_{js}^p, \delta_s$), all of which are assumed independent and normally distributed. The remainder of this section details the specification of pivotality, the functional form linking effort to turnout, and the algorithm used to compute the maximum likelihood estimates.

4.2 Perceived Voting Efficacy

In large electorates, the true probability of casting a decisive vote is negligible. Yet many models of voter turnout argue that competition itself is a key driver of turnout. To preserve this behavioral mechanism without relying on literal pivot probabilities, I model perceived voting efficacy as an endogenous function that captures how competitive a race feels to voters.

Crucially, perceived efficacy is not externally imposed. Instead, it emerges from the equilibrium of the model. The closeness of the race depends on candidate effort and voter turnout, both of which respond to voting efficacy. This feedback loop links beliefs, behavior, and strategy in a coherent structural framework.

To flexibly capture how voters internalize competitiveness, I specify the pivotality function as a two-parameter Kumaraswamy cumulative distribution:

$$p(\sigma_{s,D}, \sigma_{s,R}) = 1 - (1 - \sigma_s^{\alpha_1})^{\alpha_2}, \quad \alpha_1 > 0, \alpha_2 > 0, \quad (10)$$

where

$$\sigma_s = \begin{cases} \frac{\sigma_{s,D}}{\sigma_{s,R}}, & \text{if } \sigma_{s,R} > \sigma_{s,D}, \\ \frac{\sigma_{s,R}}{\sigma_{s,D}}, & \text{otherwise,} \end{cases} \quad \sigma_s \in (0, 1].$$

This specification allows the data to discipline both the shape and steepness of the perceived pivotality curve, without imposing a rigid form *ex ante*. Depending on the values of α_1 and α_2 , the function can approximate near-step thresholds or smooth logistic-like curves. Table 2 summarises how various values of the structural parameters map to perceived efficacy. As can be seen, the form can capture a wide range of shapes, from near-step functions to smooth logistic-like curves, depending on the values of α_1 and α_2 .

I normalize perceived efficacy to lie in $[0, 1]$; this rescaling affects utility levels but leaves the turnout condition invariant up to scale, preserving comparative statics.

4.3 Effect of Campaign Effort

Campaign effort enters voters' utility through a strictly concave production function that allows for both mobilization and persuasion:

$$u_p(e_{s,p}, e_{s,-p}) = \theta e_{s,p}^{1/\gamma} - \psi \theta e_{s,-p}^{1/\gamma}, \quad p \in \{D, R\}, \quad \gamma > 1, \quad \psi \in [0, 1].$$

Here, $e_{s,p}$ and $e_{s,-p}$ denote per-capita campaign spending by party p and its opponent in state s , respectively, and θ is a scale parameter. The exponent $1/\gamma \in (0, 1)$ implies diminishing marginal returns to effort. The persuasion parameter ψ governs how opponent spending offsets the utility gain from own-party mobilization.

I estimate the model over a two-dimensional grid:

$$\gamma \in \{2.0, 3.0, 4.0, 5.0\}, \quad \psi \in \{0.0, 0.1, 0.25, 0.5, 0.75, 1.0\}.$$

The best-fitting specification occurs at $\gamma = 2$ and $\psi = 0$, implying a square-root response function and ruling out persuasive effects of opponent spending.

Accordingly, the final model adopts a pure mobilization specification:

$$u_p(e_{s,p}) = \theta e_{s,p}^{1/\gamma}, \quad p \in \{D, R\}, \quad \gamma > 1. \quad (11)$$

This form applies exclusively to co-partisans. spending increases the utility of voters already predisposed to support party p , without affecting those aligned with the opposition. Alternative specifications that allowed cross-party persuasion consistently yielded lower likelihoods, suggesting that the data favor a model in which effort activates supporters rather than converts opponents.

4.4 Parameters

Table 2 summarises the structural parameters (Θ) and shows how each is recovered from the estimated coefficient vector β . County-level covariates X_{μ,j_s} and X_{c,j_s} capture partisanship fundamentals (e.g. race, education) and voting costs (e.g. polling-place congestion, mail-in availability), respectively. Log-parameterisation ($\exp\{\cdot\}$) ensures that costs, scale parameters, and variances remain strictly positive.

The campaign-effort parameters θ and γ jointly govern how spending translates into voter utility. I estimate θ conditional on each value of γ over a discrete grid, and select the pair that maximizes the likelihood. The final model uses $\gamma = 2$, implying a square-root response function and $\theta = 0$, indicating that campaign spending directly mobilizes supporters without cross-party persuasion.

Table 2: Structural parameters and their link to estimated coefficients

Parameter	Economic interpretation	Mapping from β
<i>Baseline utilities</i>		
μ_{j_s}	Baseline utility advantage of R in county j_s	$\beta_{\mu}^{\top} X_{\mu,j_s}$
c_{j_s}	Cost of voting in county j_s	$\exp(\beta_c^{\top} X_{c,j_s})$
<i>Perceived efficacy</i>		
α_1	Kumaraswamy shape (lower tail)	$\exp(\beta_{\alpha_1})$
α_2	Kumaraswamy shape (upper tail)	$\exp(\beta_{\alpha_2})$
<i>Campaign-effort technology</i>		
θ	Scale of utility gain per \$ spent	$\exp(\beta_{\theta})$, conditional on γ
γ	Inverse elasticity of campaign production	Grid search: $\gamma \in \{2, 3, 4, 5\}$
ψ	Persuasion parameter	Grid search: $\psi \in \{0.0, 0.1, 0.25, 0.5, 0.75, 1.0\}$
<i>Aggregate shocks</i>		
σ_{η}	Std. dev. of county-level shock	$\exp(\beta_{\eta})$
σ_{δ}	Std. dev. of state-level shock	$\exp(\beta_{\delta})$

Note: All exponentiated mappings impose positivity via log-parameterisation. Covariates in X_{μ} include demographic composition and urbanisation. Covariates in X_c include polling-place congestion, mail-in options, voter ID laws, median income, and employment rate. The parameter θ is estimated conditional on each value of γ , which is selected via grid search to maximize the likelihood.

4.5 Estimation Procedure

The structural parameters are estimated by maximum likelihood.⁹ The estimation procedure maps observables $\{\sigma_{j_s D}, \sigma_{j_s R}\}$ into the Normal shocks $\eta_{j_s}, \eta_{j_s}^p, \delta_s$,

⁹Throughout I suppress the time index t and treat a single election as given. The same procedure is repeated independently for each election in the panel. Covariates for μ are treated as unique for each year, while those for c are held fixed across time. The idea is that

which then enter the log-likelihood.

For county j in state s , under an interior solution, the observed Democratic and Republican turnout shares satisfy:

$$\begin{aligned}\sigma_{j_s D} &= H\left(u(e_{sD}, e_{sR}) - \mu_{j_s} - \frac{c_{j_s}}{p(\sigma_{sD}, \sigma_{sR})} + \eta_{j_s} + \delta_s - \eta_{j_s}^p\right), \\ \sigma_{j_s R} &= H\left(u(e_{sD}, e_{sR}) + \mu_{j_s} - \frac{c_{j_s}}{p(\sigma_{sD}, \sigma_{sR})} - \eta_{j_s} - \delta_s - \eta_{j_s}^p\right),\end{aligned}$$

where $H(\cdot)$ is the standard Normal CDF.

Taking the inverse of the CDF isolates the relevant latent thresholds:

$$H^{-1}(\sigma_{j_s D}) = u_D - \mu_{j_s} - \frac{c_{j_s}}{p} + \eta_{j_s} + \delta_s - \eta_{j_s}^p, \quad (12)$$

$$H^{-1}(\sigma_{j_s R}) = u_R + \mu_{j_s} - \frac{c_{j_s}}{p} - \eta_{j_s} - \delta_s - \eta_{j_s}^p. \quad (13)$$

Adding and subtracting these expressions yields closed-form decompositions for the county-level pivotal-shock $\eta_{j_s}^p$ and the combined county and state preference shock $\eta_{j_s} + \delta_s$:

$$\eta_{j_s}^p = \frac{1}{2} \left[-H^{-1}(\sigma_{j_s D}) - H^{-1}(\sigma_{j_s R}) + u_D + u_R - 2\frac{c_{j_s}}{p} \right], \quad (14)$$

$$\eta_{j_s} + \delta_s = \frac{1}{2} \left[H^{-1}(\sigma_{j_s D}) - H^{-1}(\sigma_{j_s R}) - u_D + u_R + 2\mu_{j_s} \right]. \quad (15)$$

Since η_{j_s} is i.i.d. with mean zero, averaging (15) across counties in state s provides an unbiased estimator for the state-level preference shock:

$$\hat{\delta}_s = \frac{1}{|J_s|} \sum_{j_s} \frac{1}{2} \left[H^{-1}(\sigma_{j_s D}) - H^{-1}(\sigma_{j_s R}) - u_D + u_R + 2\mu_{j_s} \right].$$

Subtracting $\hat{\delta}_s$ from (15) recovers the county-specific deviation $\hat{\eta}_{j_s}$.

Therefore, given a parameter vector Θ , the implied shocks $\hat{\eta}_{j_s}, \eta_{j_s}^p, \hat{\delta}_s$ are uniquely determined by the data. Under the maintained assumption that $\eta, \eta^p \sim \mathcal{N}(0, \sigma_\eta^2)$ and $\delta \sim \mathcal{N}(0, \sigma_\delta^2)$, the log-likelihood is the sum of Gaussian densities evaluated at these shocks.

I maximize the likelihood using the Adam algorithm. At each iteration, for a candidate value of the parameter vector Θ , I solve a nested fixed-point system to evaluate the corresponding log-likelihood.

This system has two levels:

1. **Campaign equilibrium (outer fixed point):** For given values of $\theta, \mu_{j_s}, c_{j_s}$, and the pivotality function, I solve for the equilibrium allocation of campaign efforts $\{e_{sD}, e_{sR}\}$ as described in Section 3.3.3.

election-specific candidates and issues may shift baseline utilities, whereas the institutional and logistical components of voting costs remain stable.

2. **Inner fixed point (state level):** For each swing state s and a trial effort profile (e_{sD}, e_{sR}) , I solve the three-equation system

$$(\hat{\delta}_s, \tilde{\sigma}_{s,D}, \tilde{\sigma}_{s,R}) \quad \text{such that} \quad \begin{cases} \sum_{j_s} w_{j_s} H\left(u(e_{s,D}) - \mu_{j_s} - \frac{c_{j_s}}{p(\tilde{\sigma}_{s,D}, \tilde{\sigma}_{s,R})} + \hat{\delta}_s\right) \\ = \sum_{j_s} w_{j_s} H\left(u(e_{s,R}) + \mu_{j_s} - \frac{c_{j_s}}{p(\tilde{\sigma}_{s,D}, \tilde{\sigma}_{s,R})} - \hat{\delta}_s\right) \\ \tilde{\sigma}_{s,D} = \sum_{j_s} w_{j_s} \tilde{\sigma}_{j_s,D} \\ \tilde{\sigma}_{s,R} = \sum_{j_s} w_{j_s} \tilde{\sigma}_{j_s,R} \end{cases}$$

where the county-level tilde shares $\tilde{\sigma}_{j_s,D}, \tilde{\sigma}_{j_s,R}$ suppress the idiosyncratic county shocks (see Sec. 3.3.2). The resulting triplet yields the approximated probability of D winning the state $\tilde{p}_s(e_{s,D}, e_{s,R}) = 1 - F(\hat{\delta}_s)$, which feeds back into the outer equilibrium computation.

This inner-outer fixed-point system is resolved to convergence before each likelihood evaluation.

The entire procedure is repeated over a grid of curvature parameters (γ, ψ) . For each grid pair, I maximize the likelihood over the remaining parameters in Θ . The final estimates correspond to the parameter configuration that yields the highest log-likelihood across all grid points.

4.6 Identification and Monte-Carlo Validation

To check the identification of the structural parameters, I conduct a Monte-Carlo simulation exercise where I use the actual data though draw random coefficients that are then mapped into the structural parameters. I then attempt to recover these coefficients following the estimation procedure used in the empirical application.

In each of the $R = 100$ replications, I hold fixed county- and state-level covariates observed in the real data, $(X_{j_s}^\mu, X_{j_s}^c)$, and draw a fresh vector of coefficients

$$(\beta_\mu, \beta_c, \beta_{\alpha_1}, \beta_{\alpha_2}, \beta_\theta, \beta_\eta, \beta_\delta)$$

¹⁰ Given the parameters and coefficients, I compute the equilibrium campaign efforts $(e_{s,D}^{(r)}, e_{s,R}^{(r)})$ and the corresponding turnout rates after drawing county- and state-level shocks. Finally, I re-estimate the model on this synthetic election using the likelihood function and optimisation routine applied to the actual data.

For some simulations, the candidate-side subroutine fails to compute an equilibrium effort profile. Since this issue does not arise in the empirical application, I exclude these draws from the analysis. I also discard simulations where the likelihood-based estimator fails to converge within a pre-specified iteration limit. This cap acts as a time-out to keep the Monte-Carlo procedure tractable.

¹⁰To economise on computation time, I work with a reduced covariate set and fix $\gamma = 2$ and $\psi = 0$.

Figure 1 visualises the distribution of $\hat{\beta}_j - \beta_j^{\text{true}}$ across the convergent replications. Table 3 reports the mean and standard deviation of this difference for the estimated coefficients. Across the estimated coefficients, the average root-mean-squared error (RMSE) is .015, with the largest RMSE of .0665 for the county-level shock variance σ_η . Even for the relatively noisy variance parameters, the 95-percent simulation interval of the estimation error is centred at zero. Taken together, the Monte-Carlo evidence confirms that the likelihood surface is sufficiently informative to pin down the full vector of structural parameters.

Table 3: Parameter-recovery diagnostics across Monte-Carlo replications

Parameter	MSE	RMSE	2.5th pctl	97.5th pctl
Male (18–29)	2.37×10^{-5}	0.00487	−0.0085	0.0095
Female (65–79)	6.66×10^{-5}	0.00816	−0.0158	0.0123
White	2.50×10^{-6}	0.00158	−0.0032	0.0032
Black	3.60×10^{-6}	0.00190	−0.0028	0.0043
Hispanic	4.60×10^{-6}	0.00214	−0.0038	0.0032
High school only	1.50×10^{-5}	0.00387	−0.0068	0.0066
Some college	1.12×10^{-5}	0.00335	−0.0037	0.0066
College only	1.73×10^{-5}	0.00416	−0.0079	0.0081
College+	2.53×10^{-5}	0.00503	−0.0060	0.0013
Employed	2.69×10^{-5}	0.00519	−0.0019	0.0030
Voter ID Index	2.51×10^{-7}	0.00050	−0.00047	0.00044
α_1	0.00094	0.0307	−0.0458	0.0029
α_2	0.00108	0.0329	−0.0472	0.0030
θ	3.21×10^{-6}	0.00179	−0.0020	0.0020
σ_η	0.00442	0.0665	−0.0129	0.0742
σ_δ	0.00387	0.0622	−0.0730	0.169

Notes: MSE is the mean squared estimation error across Monte-Carlo replications, and RMSE is its square root. The final two columns report the 2.5th and 97.5th percentiles of the estimation error distribution for each parameter.

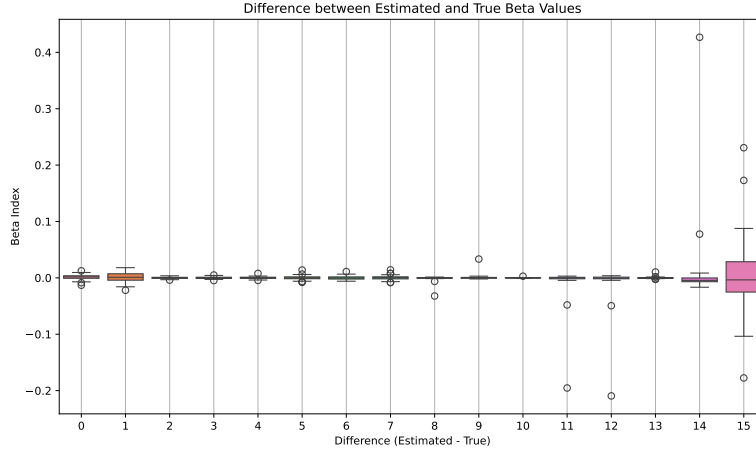


Figure 1: Distribution of estimation error ($\hat{\beta}_j - \beta_j^{\text{true}}$) across 100 simulated data sets. Each box summarises one coefficient; whiskers span the 5th–95th percentiles. The dotted line at zero marks perfect recovery.

5 Data

The empirical analysis combines county-election information for the 2008, 2012, 2016, and 2020 presidential cycles. Five public sources are merged to obtain (i) official vote totals, (ii) demographic data, (iii) proxies for the cost of voting, and (iv) campaign budgets. The resulting panel contains 12,225 county-election observations after minimal sample restrictions described below.

5.1 Voting Data

County-level Democratic and Republican vote counts are taken from the MIT Election Data and Science Lab’s harmonized returns. Table 4 summarizes turnout rates by party and geography, disaggregating between county- and state-level aggregates and between battleground and non-battleground states. Two patterns emerge.

First, turnout varies far more at the county level than at the state level, reflecting substantial within-state heterogeneity in partisanship, salience, and voting conditions. This motivates the use of county-level data. Because pivotality and campaign effort are assigned at the state level, counties within a state share the same strategic environment. This structure provides a rich source of identification as it allows the model to compare turnout across counties with identical pivotality and campaign intensity but differing in demographics and voting costs. Observing many such counties helps separately identify the role of baseline utilities, cost shifters, and unobserved shocks in shaping turnout behavior.

Second, state-level turnout is more dispersed in non-battleground states than in battlegrounds. The standard deviation of Democratic turnout across states is 0.098 in non-battlegrounds, compared to just 0.038 in battlegrounds, and for Republicans, the standard deviations are 0.117 and 0.027, respectively. This pattern is consistent with the mechanisms embedded in the model: in more competitive states, higher pivotality and targeted campaign effort both act to raise turnout. As a result, battleground states exhibit not only higher average participation, but also more uniform turnout across states, relative to non-battlegrounds where effort is absent and competitiveness varies more widely.

Table 4: Turnout Summary Statistics by Geography and State Type

Level	Party	Battleground States		Non-Battleground States	
		Mean	Std. Dev.	Mean	Std. Dev.
County	Democrat	0.260	0.093	0.203	0.102
	Republican	0.362	0.097	0.369	0.117
State	Democrat	0.321	0.038	0.262	0.098
	Republican	0.307	0.027	0.275	0.092

Note: County-level figures are unweighted averages across counties; state-level figures reflect aggregated state totals. Turnout is defined as the fraction of eligible voters casting a ballot for each party.

5.2 Demographics Data

Demographic covariates come from the five-year American Community Survey (ACS). For each election t I use the ACS file whose midpoint year equals t , thereby maximising sample size while maintaining temporal alignment.¹¹ All monetary variables are expressed in 2020 dollars using the CPI-U.¹² I additionally calculate the density of the county by taking the land area in kilometers squared and dividing it by the number of residents. I use this to classify counties as urban or rural, with the cutoff set at 350 residents per square kilometer.¹³ I drop any county-election cell with missing vote totals or demographic information. Further, I drop counties with 500 or fewer residents, as often these areas report more than 100 percent turnout due to small numbers of votes and registered voters. Tables 5 and 6 present summary statistics for the demographic covariates used in the analysis, split by battleground and non-battleground states.

¹¹For example, the 2006-10 ACS file is matched to the 2008 election.

¹²Data is available from <https://fred.stlouisfed.org/series/CPIAUCSL>

¹³This threshold is chosen to match the classification rule used by the U.S. Census Bureau which used 1,000 residents per square mile. <https://www.census.gov/newsroom/blogs/random-samplings/2022/12/redefining-urban-areas-following-2020-census.html>

Table 5: Summary Statistics for Covariates Used in the Partisan-Bias Parameter (Battleground States)

Variable	Count	Mean	Std. Dev.	Min	25%	50%	75%	Max
Male	3,174	0.501	0.026	0.374	0.488	0.496	0.505	0.790
Age 18–29	3,174	0.147	0.047	0.034	0.123	0.137	0.156	0.591
Age 65+	3,174	0.162	0.044	0.028	0.134	0.159	0.185	0.514
White	3,174	0.789	0.176	0.086	0.680	0.852	0.932	0.998
Black	3,174	0.103	0.143	0.000	0.008	0.033	0.145	0.791
Native American	3,174	0.008	0.037	0.000	0.001	0.002	0.004	0.796
Asian	3,174	0.013	0.018	0.000	0.003	0.006	0.014	0.189
Hispanic	3,174	0.066	0.082	0.000	0.019	0.039	0.078	0.831
High School Only	3,174	0.352	0.077	0.055	0.304	0.354	0.405	0.556
Some College	3,174	0.297	0.048	0.114	0.265	0.300	0.330	0.455
College Only	3,174	0.142	0.059	0.030	0.098	0.130	0.170	0.480
College+	3,174	0.077	0.046	0.007	0.047	0.064	0.094	0.437
Log Pop. Density	3,174	0.400	0.081	0.105	0.349	0.393	0.447	1.000

Note: All variables are expressed as population shares unless otherwise noted. Density and income variables are normalized to the unit interval using empirical percentiles. Statistics are based on county-level data from swing states where effort is endogenously allocated in equilibrium.

Table 6: Summary Statistics for Covariates Used in the Partisan-Bias Parameter (Non-Battleground States)

Variable	Count	Mean	Std. Dev.	Min	25%	50%	75%	Max
Male	9,322	0.501	0.023	0.405	0.489	0.497	0.507	0.764
Age 18–29	9,322	0.147	0.041	0.031	0.125	0.141	0.159	0.554
Age 65+	9,322	0.157	0.041	0.031	0.129	0.154	0.181	0.402
White	9,322	0.763	0.207	0.007	0.647	0.839	0.927	1.000
Black	9,322	0.084	0.144	0.000	0.005	0.018	0.085	0.874
Native American	9,322	0.021	0.081	0.000	0.001	0.003	0.007	0.910
Asian	9,322	0.013	0.030	0.000	0.002	0.005	0.011	0.522
Hispanic	9,322	0.097	0.148	0.000	0.020	0.038	0.098	0.991
High School Only	9,322	0.345	0.070	0.071	0.300	0.349	0.396	0.557
Some College	9,322	0.301	0.055	0.111	0.265	0.301	0.338	0.506
College Only	9,322	0.136	0.055	0.019	0.095	0.126	0.166	0.457
College+	9,322	0.072	0.042	0.000	0.045	0.060	0.086	0.483
Log Pop. Density	9,322	0.359	0.092	0.000	0.305	0.362	0.410	0.755

Note: All variables are expressed as fractions of county population unless otherwise noted. Density and income variables are normalized to the unit interval using empirical percentiles. Observations cover counties in non-battleground states where campaign effort is exogenously set to zero in equilibrium.

5.3 Cost of Voting

Polling-place congestion. I proxy queues at the polls with a crowding index that scales the voting-age population by the number of in-person polling locations on Election Day. Let PP_{jt} denote the number of polling places and

VAP_{jt} the voting-age population in county j during election year t , defined as the number of residents aged 18 and older. The congestion index is defined as

$$Congest_{jt} = \log \left(\frac{VAP_{jt}}{\widehat{PP}_{jt}} \right),$$

where \widehat{PP}_{jt} is the observed number of polling sites, or a predicted value when the data is missing.

Polling place data come from the Election Administration and Voting Survey (EAVS), a biennial national survey administered by the U.S. Election Assistance Commission. The EAVS collects detailed administrative data from local election officials, including the number of polling places, voting methods, and ballots cast. However, approximately 19% of county-election observations are missing polling place data.

I impute these missing values using a Gradient Boosting model trained on county-year covariates, including a linear time trend, log voting-age population, demographic shares (age, gender, race, education, employment), and state fixed effects. I first log-transform the number of polling places to reduce skewness and ensure positive predictions. Model hyperparameters are selected via five-fold cross-validated grid search over tree depth, regularization, learning rate, and number of iterations. The model is trained on observed data from the 2008-2020 cycles. The final model achieves an out-of-sample $R^2 = 0.838$.

To match the scale of other covariates, I convert $Congest_{jt}$ to its empirical percentile. Motivated by evidence that urban and rural residents experience polling-places differently (Bagwe, Margitic, and Stashko 2022), I interact the congestion index with an indicator for urban status, defined as counties with more than 350 residents per square kilometer. This yields two separate covariates: one for urban congestion and one for rural congestion. Finally, in states that conduct universal vote-by-mail, I set the congestion index to zero. Summary statistics for the polling-place congestion index are presented in Table 7. Table 7 shows the summary statistics for percentile-transformed congestion measures, separating urban and rural counties in battleground and non-battleground states.

Table 7: Summary Statistics for Cost of Voting Index by Urban/Rural Status and State Type

Statistic	Urban Counties		Rural Counties	
	BG	Non-BG	BG	Non-BG
Count	231.000	375.000	2880.000	8324.000
Mean	0.584	0.593	0.540	0.521
Std. Dev.	0.042	0.050	0.054	0.064
Min	0.471	0.491	0.334	0.000
25th Pctl	0.559	0.563	0.505	0.482
Median	0.590	0.587	0.536	0.519
75th Pctl	0.609	0.613	0.570	0.558
Max	0.760	0.976	0.887	1.000

Note: The cost of voting index reflects percentile-transformed congestion measures interacted with urban status. Urban counties are defined as those with more than 350 residents per square kilometer. BG = Battleground states (receive campaign effort); Non-BG = Non-battleground states (no campaign effort). All statistics are computed at the county-election level. Values are at the county-election level.

Election-law cost shifters. To capture cross-state and temporal variation in the administrative burden of voting, I incorporate three state-level measures from Li, Pomante, and Schraufnagel (2018). First, voter identification (ID) requirements are coded on a five-point scale ranging from 0 (signature only) to 4 (strictly enforced photo ID), with intermediate values for less stringent enforcement and non-photo alternatives. Second, polling access is proxied by the statutory number of in-person voting hours on Election Day. Li, Pomante, and Schraufnagel (2018) compute each state’s average from the minimum and maximum legal polling times and subtract this value from 20—the maximum feasible window from midnight to 8:00 p.m. to define a *poll-hours gap*. For mail-in voting states, HI, UT, and CO are scored based on actual polling hours since they maintain physical polling places, while OR and WA are assigned the full 20-hour window based on ballot return deadlines. Third, registration deadlines are measured as the number of days before Election Day by which voters must register; states offering same-day registration receive a score of zero.

In all cases, I apply a linear transformation subtracting the minimum and dividing by the range to map the raw values from Li, Pomante, and Schraufnagel (2018) to the unit interval $[0, 1]$, where higher scores correspond to more restrictive policies. This transformation ensures that these election-law cost shifters are on the same scale as the demographic and congestion covariates, making them easier to estimate alongside the other parameters in the model.

Table 8: Summary Statistics for Election-Law Indices by State Type

Statistic	Voter ID Index		Poll Hours Index		Reg. Deadline Index	
	BG	Non-BG	BG	Non-BG	BG	Non-BG
Count	40	160	40	160	40	160
Mean	0.300	0.273	0.377	0.380	0.519	0.563
Std. Dev.	0.345	0.317	0.142	0.207	0.463	0.406
Min	0.000	0.000	0.000	0.000	0.000	0.000
25th Pctl	0.000	0.000	0.333	0.333	0.000	0.000
Median	0.250	0.250	0.333	0.417	0.717	0.700
75th Pctl	0.500	0.500	0.500	0.500	0.967	0.967
Max	1.000	1.000	0.667	1.000	1.000	1.000

Note: All indices are scaled to the unit interval. Higher values reflect more restrictive voting policies. BG = Battleground states (receive campaign effort); Non-BG = Non-battleground states (no campaign effort). Values is at the state-year level.

Income and employment. To account for the opportunity cost of time and broader economic constraints, I include two covariates at the county-election level: real median household income and the share of the voting-age population that is employed. Real income is expressed in 2020 dollars and normalized to the unit interval using empirical percentiles, as described in Section 5.2. Employment shares are calculated directly from American Community Survey data.

Table 9 presents summary statistics for these variables, split by battleground and non-battleground states. Counties in battleground states tend to have slightly higher real income and employment levels on average, and with less variation, compared to non-battleground states.

Table 9: Summary Statistics for Cost of Voting Covariates by State Type

Statistic	Log Real Median HH Income (frac)		Fraction Employed	
	BG	Non-BG	BG	Non-BG
Count	3,174	9,059	3,174	9,059
Mean	0.907	0.903	0.598	0.589
Std. Dev.	0.020	0.035	0.080	0.079
Min	0.839	0.000	0.136	0.000
25th Pctl	0.894	0.890	0.551	0.541
Median	0.906	0.903	0.606	0.597
75th Pctl	0.920	0.916	0.654	0.645
Max	0.988	1.000	0.855	0.831

Note: All variables are normalized to the unit interval using empirical percentiles. BG = Battleground states (receive campaign effort); Non-BG = Non-battleground states (no campaign effort). Statistics are based on county-election level observations.

Table 10: Summary Statistics for Estimated Cost of Voting by State Type

Statistic	Cost		Cost (Pivotality-Adjusted)	
	BG	Non-BG	BG	Non-BG
Mean	0.582	0.594	0.583	0.618
Std. Dev.	0.0727	0.0713	0.0728	0.0769
Min	0.329	0.321	0.330	0.324
Max	0.813	0.824	0.813	0.892

Note: Cost is computed as $c_{js} = \exp(\beta_c \cdot X_{js}^{(c)})$. The pivotality-adjusted cost, $c_{js}/p(\sigma_{s,D}, \sigma_{s,R})$, appears in the turnout equations for both parties (equations (1)–(2)) and reflects the effective cost of voting after scaling by perceived pivotality at the state level. Higher values of p (i.e., greater competitiveness) reduce the deterrent effect of voting costs. BG = Battleground states; Non-BG = Non-battleground states.

5.4 Identifying Battleground States and Constructing Campaign Effort

While the model endogenously determines how effort is allocated across states, I must first identify which states are contested and quantify the total campaign resources available to each party in each election year. I define battleground states empirically using data from the Wesleyan Media Project, which reports state-level television advertising by party and sponsor type. I then use national disbursement records from the Federal Election Commission (FEC) to scale these observed media expenditures into a broader measure of total mobilization effort within each battleground state. Summing across states yields the total campaign budget available to each party in each election year. Later, in Section 6.7, I validate that the model’s predicted effort allocations align closely with observed campaign behavior.

I define battleground states as the ten states with the highest combined Democratic and Republican television advertising expenditures in each presidential election cycle. For this, I use state-level data from the Wesleyan Media Project, which tracks television advertising by party and sponsor type from 2008 to 2020. All spending figures are deflated to 2020 dollars using the Consumer Price Index (CPI-U). The battleground classification is recalculated separately for each election year. As shown in Figure 2, these states consistently receive the bulk of campaign activity, highlighting their strategic centrality to presidential contests.

While the Wesleyan Media Project provides detailed data on television advertising within battleground states, it does not capture the full scope of campaign mobilization. Television is a key channel, but campaigns also engage in digital outreach, direct mail, telemarketing, and travel, with meaningful variation across parties in how resources are allocated. Relying solely on television data would understate total campaign effort, and could bias comparisons if one party disproportionately invests in non-television channels.

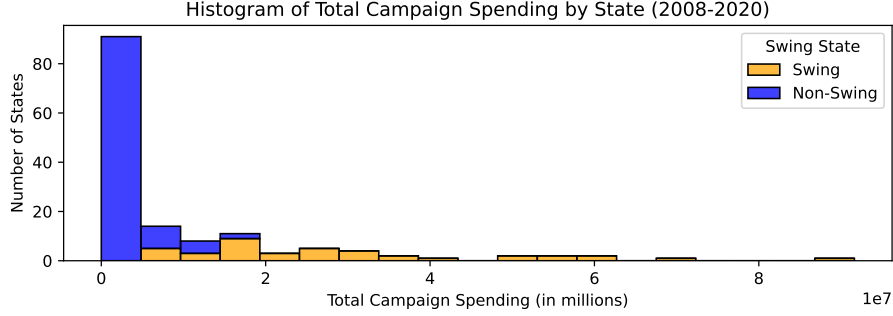


Figure 2: Distribution of Total Campaign Spending in Battleground vs. Non-Battleground States. The histogram shows total campaign spending in battleground states (orange) and non-battleground states (blue) for each election year from 2008 to 2020. The y-axis represents the number of states in each bin, while the x-axis shows total spending in millions of dollars.

To address this, I use the Wesleyan data as a base to identify mobilization efforts within battleground states, and then scale these figures to recover total campaign budgets. This is done using Federal Election Commission (FEC) itemized disbursement records, which provide a comprehensive view of campaign spending by category.

Although the FEC includes purpose descriptions for each transaction, it does not report where the activity occurs. Vendor addresses are recorded, but reflect the firm’s location, not the target of mobilization. For instance, an advertising agency based in California may deploy ads in Michigan.

To isolate direct voter contact, I classify each transaction into one of five mutually exclusive mobilization categories—media, digital, print, telemarketing, and travel— based on keyword matching in the purpose description field (see Appendix C). This procedure excludes overhead expenditures such as salaries, legal fees, and compliance costs.

Let $\text{FEC}_{p,t,c}$ denote total spending by party p in category c during year t . I compute the national share of spending allocated to each category as:

$$\phi_{p,t,c} = \frac{\text{FEC}_{p,t,c}}{\sum_c \text{FEC}_{p,t,c}}.$$

Assuming that television ads correspond to the “media” category, I infer total effort in battleground state s as:

$$E_{s,p,t} = \frac{\text{TV}_{s,p,t}}{\phi_{p,t,\text{media}}},$$

and total party-level effort as:

$$E_{p,t} = \sum_{s \in BG_t} E_{s,p,t}.$$

Table 11 reports the estimated composition of campaign disbursements. Table 12 shows total inferred mobilization budgets by party and year, aggregated over battleground states.

To isolate general-election activity, I restrict the Wesleyan sample to ads aired on or after August 1 of each election year. By this point, major-party nominees are finalized, primaries are complete, and campaigns begin targeting the general electorate.

Table 11: Share of Disbursements by Category and Party

Category	2008		2012		2016		2020	
	Dem	Rep	Dem	Rep	Dem	Rep	Dem	Rep
Media	0.704	0.774	0.744	0.674	0.772	0.431	0.615	0.472
Online / digital	0.079	0.000	0.108	0.123	0.073	0.387	0.367	0.441
Print / mail	0.060	0.025	0.035	0.055	0.005	0.010	0.003	0.022
Phone / text	0.024	0.068	0.047	0.044	0.004	0.009	0.004	0.000
Travel / event	0.133	0.133	0.066	0.105	0.145	0.164	0.011	0.064

Notes: Entries report the fraction of total *itemized operating disbursements* made by the two major-party presidential candidate committees that falls in each spending category during the indicated election cycle. Shares are calculated from Federal Election Commission (FEC) operating-expenditure files after (i) restricting to general-election spending by the principal presidential committees, and (ii) assigning each transaction to a single category using keyword matching (see Appendix C for details). Columns sum to one within each party-year.

Table 12: Total Campaign Spending in Swing States by Party (2020 USD)

Year	2008	2012	2016	2020
Democratic	257,000,000	349,000,000	153,000,000	392,000,000
Republican	158,000,000	221,000,000	155,000,000	416,000,000

Notes: Total estimated campaign expenditures in swing states, aggregated at the party level. Values are in constant 2020 dollars and reflect the inferred mobilization budget $B_{s,p}$ constructed from television advertising data and scaled using national disbursement shares.

6 Results

Figure 3 and Table 13 summarize the estimated coefficients, illustrating how demographic composition and institutional features shape both baseline political alignment and the cost of voting.¹⁴ The table also includes coefficients associated with the utility gain from campaign effort, the perceived voting efficacy, and the county- and state-level shocks that capture unobserved heterogeneity.

¹⁴For ease of interpretation, coefficients for the μ component are shown graphically in Figure 3, while the full set of estimates appears in Table 22 in the Appendix.

6.1 Estimated Coefficients for Partisan Alignment

The μ coefficients govern counties' baseline political alignment ($\mu_{j_s} = \beta_\mu \cdot X_{j_s}^\mu$) where $X_{j,s}^\mu$ is a vector of county-level demographic and socio-economic variables. Negative values shift counties toward a Democratic baseline, while positive values shift them toward a Republican baseline. Figure 3 shows the estimated coefficients for the μ component, along with 95% confidence intervals. As can be seen, most coefficients are statistically different from zero. Further, the signs align with well-established empirical patterns. Counties with higher rates of college or advanced degree attainment, and larger Black and Hispanic population shares, lean more Democratic. In contrast, counties with higher proportions of white residents or lower educational attainment tend to lean more Republican. Further, more dense counties tend to lean more Democratic, suggesting that urbanization is a strong predictor of partisan alignment. These results serve as a useful validity check on the model's estimates.

6.2 Estimated Coefficients for the Cost of Voting

Table 13 reports how institutional and socio-economic variables affect the cost of voting. The cost function is specified as $c_{j_s} = \exp(\beta_c \cdot X_{j_s}^{(c)})$. Positive coefficients indicate that higher values of the variable increase the cost of voting; negative coefficients indicate cost reductions.

Polling Place Congestion The two congestion measures, separated by urban and rural areas, are both large and statistically significant. Moving from the lowest to highest decile of the urban congestion distribution raises $\beta_c \cdot X_c$ by approximately 0.58; in rural areas, the comparable increase is 0.46. To better understand the implications of these coefficients, I calculate the elasticity of turnout with respect to congestion.

Table 14 reports these results, averaged across counties in battleground states. A 1% increase in urban congestion reduces Democratic turnout by 0.20% and Republican turnout by 0.17%, while a 1% increase in rural congestion lowers turnout by 0.12% and 0.13%, respectively. These estimates show that congestion meaningfully depresses participation, with effects somewhat larger in urban settings.

Institutional Barriers Three additional variables capture formal voting rules that shape the ease of participation: voter identification requirements, poll hours, and registration deadlines. The coefficient on Registration Deadlines is positive, statistically significant, and relatively large (0.178, $p < 0.001$), indicating that longer pre-election registration windows impose a meaningful participation cost. This aligns with findings in the literature showing that reducing registration frictions can meaningfully raise turnout (Grumbach and C. Hill 2022; Burden et al. 2014).

By contrast, Voter ID Laws (0.003, $p = 0.633$) and Poll Hours (-0.009 , $p = 0.559$) are both small and statistically insignificant. The null effect of

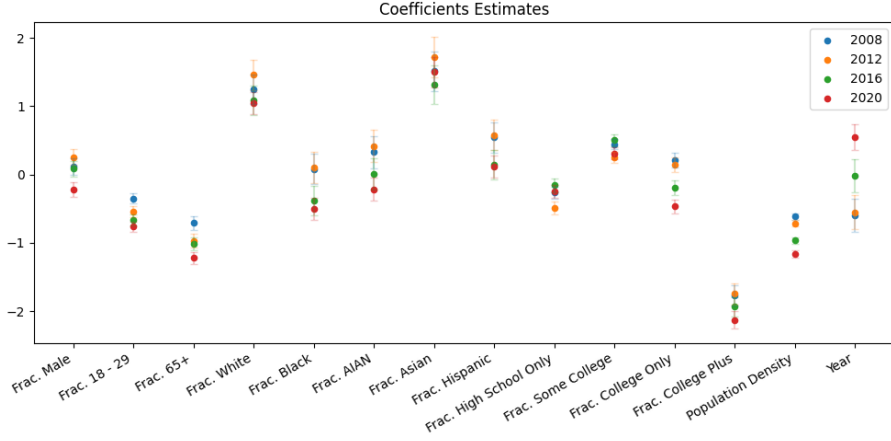


Figure 3: Estimated Coefficients entering the μ component for the Model. The plot shows the estimated coefficients for the model, with 95% confidence intervals. The coefficients represent the impact of various factors on the political alignment of counties and the cost of voting. Population Density is log-transformed and standardized to the 0-1 range.

voter ID laws aligns with recent empirical work showing limited turnout effects (Cantoni and Pons 2021).

Elasticity estimates confirm these patterns. A 1% increase in the registration deadline raises turnout by 0.08% for Democrats and 0.09% for Republicans (Table 14). In contrast, the elasticities for voter ID and poll hours are near zero.

Socio-Economic Factors The final two covariates, Median Household Income and Fraction Employed, capture how economic resources affect the ease of voting. Both coefficients are large in magnitude, negative, and highly statistically significant ($p < 0.001$), implying that counties with higher income levels and employment rates experience substantially lower effective costs of turnout.

Table 13: Estimated Coefficients

Parameter	Variable	Coefficient	Standard Error	P-Value
<i>Cost of Voting</i>				
	Constant	1.931	0.103	0.000
	Congestion (Urban)	0.584	0.027	0.000
	Congestion (Rural)	0.458	0.024	0.000
	Voter ID Laws	0.003	0.006	0.633
	Employment Rate	-0.163	0.034	0.000
	Registration Deadlines	0.178	0.006	0.000
	Median HH Income	-3.005	0.126	0.000
	Poll Hours	-0.009	0.015	0.559
<i>Voting Efficacy</i>				
	Constant 1	0.075	0.079	0.348
	Constant 2	1.241	0.094	0.000
<i>Campaign Effort</i>				
	θ	-3.120	0.034	0.000
<i>County and State-level Shocks</i>				
	σ_η	-2.031	0.005	0.000
	σ_δ	-1.564	0.059	0.000

Notes: All coefficients are from the maximum likelihood estimation. Cost-related covariates are expressed in standardized units (e.g., percentiles or logs). The shock parameters are reported in log standard deviation units. P-values are based on robust standard errors clustered at the state level.

Table 14: Mean Elasticity of Turnout with Respect to Cost Variables

Variable	Turnout (D)	Turnout (R)
<i>Cost of Voting</i>		
Congestion (Urban)	-0.200	-0.174
Congestion (Rural)	-0.117	-0.131
Voter ID Laws	-0.001	-0.001
Registration Deadlines	-0.077	-0.088
Poll Hours	0.003	0.004
Median HH Income	1.425	1.564
Employment Rate	0.029	0.031

Note: Entries report the mean elasticity of Democratic and Republican turnout with respect to each cost-related covariate. Elasticities are defined as $\varepsilon_{j,p} = (\partial\sigma_{j,p}/\partial x_j)(x_j/\sigma_{j,p})$, averaged over counties in battleground states.

6.3 County-Level Political Alignment

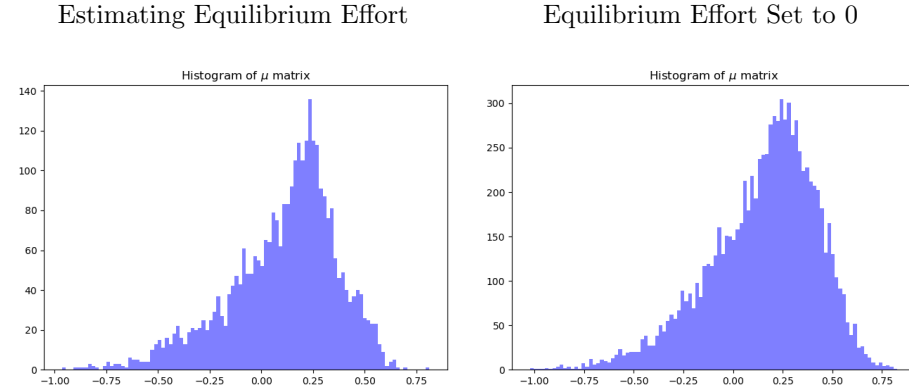
Figure 4 shows the estimated distribution of μ_{j_s} , which captures each county's baseline partisan alignment. Formally, μ_{j_s} represents the expected utility differential favoring the Republican candidate in county j of state s , prior to the realization of campaign effort or any county- or state-level shocks.

The left panel of Figure 4 plots this distribution for counties in battleground states; the right panel shows the same for non-battleground states. In both cases, the distribution is unimodal, slightly right-skewed, and centered around modestly pro-Republican values: the mean μ is 0.11 in battleground counties and 0.14 in non-battleground counties.

Because the histograms are not population-weighted, they overrepresent smaller rural counties, which tend to lean Republican, relative to densely populated urban areas that lean Democratic. As a result, the unweighted mean reflects geographic rather than electoral mass.

Interestingly, in both samples, the distribution of μ_{j_s} exhibits a longer left tail than right. While most counties lean moderately Republican, the most extreme values of μ_{j_s} , those with the strongest partisan tilt, are disproportionately Democratic.

Figure 4: Estimated μ for all counties



Note: The figures show the estimated baseline county-level utility in favor of the Republican candidate (μ_{j_s}). The left panel shows the estimated μ_{j_s} for counties in battleground-states (where equilibrium effort levels are calculated), while the right panel shows the corresponding estimates for non-battleground states. .

6.4 County-Level Cost of Voting

Figure 5 plots the estimated cost of voting across all U.S. counties, separately for battleground and non-battleground states. Table 15 summarizes the key statistics. The cost measure shown here, $c_{j_s} = \exp(\beta_c \cdot X_{j_s}^{(c)})$, reflects institutional and socioeconomic barriers to participation, but does not yet account for perceived voting efficacy. I turn to that adjustment in the next section.

In the raw cost estimates, average values are quite similar across the two groups: the mean is 0.582 in battleground counties and 0.594 in non-battlegrounds, with nearly identical dispersion (standard deviation = 0.0727 vs. 0.0713). The similarity reflects the fact that institutional voting costs, such as registration deadlines and polling congestion, do not systematically differ by state competitiveness.

However, this picture shifts once we account for perceived voting efficacy. Because efficacy is systematically lower in non-battleground states, the effective cost of voting is higher in those areas. The next subsection formalizes this adjustment and shows that, after incorporating efficacy, the gap in participation costs between battleground and non-battleground counties widens considerably.

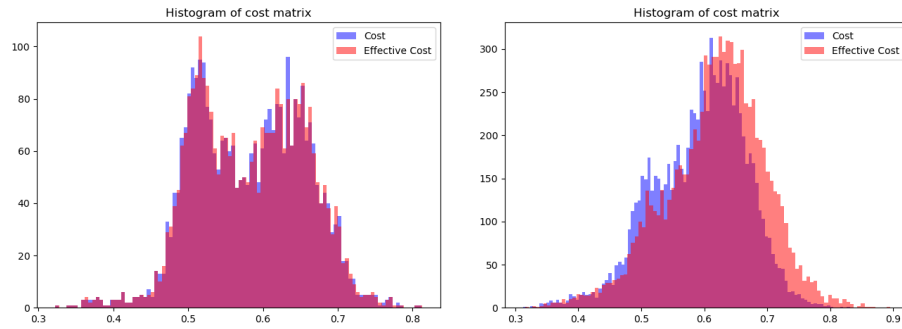
Table 15: Summary Statistics for Estimated Cost of Voting by State Type

Statistic	Cost		Effective Cost	
	BG	Non-BG	BG	Non-BG
Mean	0.582	0.594	0.583	0.618
Std. Dev.	0.0727	0.0713	0.0728	0.0769
Min	0.329	0.321	0.330	0.324
Max	0.813	0.824	0.813	0.892

Note: Raw cost is computed as $c_{js} = \exp(\beta_c \cdot X_{js}^{(c)})$. The effective cost adjusts for perceived voting efficacy, $c_{js}/p(\sigma_{s,D}, \sigma_{s,R})$, as defined in the turnout equations (Equations (1)–(2)). Lower values of p raise the effective cost, dampening turnout incentives. BG = Battleground states; Non-BG = Non-battleground states.

Figure 5: Estimated cost for all counties

Swing States (with equilibrium effort) Safe States (no campaign equilibrium)



Note: The figures show the estimated cost of voting for all counties. The left panel shows the estimates for counties where the equilibrium effort levels are calculated, while the right panel shows the corresponding estimates for non-competitive states.

6.5 Perceived Voting Efficacy

As defined in Section 3, the closeness ratio for a statewide contest is

$$\sigma_s = \begin{cases} \frac{\sigma_{s,D}}{\sigma_{s,R}}, & \text{if } \sigma_{s,R} > \sigma_{s,D}, \\ \frac{\sigma_{s,R}}{\sigma_{s,D}}, & \text{otherwise,} \end{cases} \quad \sigma_s \in (0, 1],$$

which equals one in a perfectly competitive race and approaches zero as the expected margin widens. An individual's voting efficacy is then defined as:

$$p(\sigma_s; \alpha_1, \alpha_2) = 1 - (1 - \sigma_s^{\alpha_1})^{\alpha_2}, \quad \alpha_1 > 0, \alpha_2 > 0.$$

Maximum likelihood estimation yields

$$\hat{\alpha}_1 = 1.07, \quad \hat{\alpha}_2 = 3.46,$$

implying a steep but continuous relationship between competitiveness and perceived voting efficacy. Figure 6 plots the fitted function against observed values of σ_s . The curve exceeds 0.99 by $\sigma_s \approx 0.75$, indicating that voters in moderately close contests (e.g., a 4:3 ratio) perceive themselves as nearly maximally efficacious. Even in races with $\sigma_s = 0.5$, where the leading candidate is expected to receive twice as many votes as the trailing one, perceived efficacy remains above 0.9.

Because pivotality enters the decision rule multiplicatively (see Equations (1)–(2)), even at these high levels, changes in σ_s materially affects the effective cost of voting:

$$\tilde{c}_s \equiv \frac{c_s}{p(\sigma_s)}.$$

For instance, assuming a baseline cost $c_s = 0.59$ (the mean in non-battleground states),

$$\tilde{c}_s = \begin{cases} 0.59/0.90 \approx 0.66, & \text{if } \sigma_s = 0.50, \\ 0.59/1.00 = 0.59, & \text{if } \sigma_s = 1.00, \end{cases}$$

a 12% increase in the effective cost of participation.

This adjustment is modest in battleground, where competitiveness is already high. But in non-battleground states, it meaningfully shifts the cost distribution. The mean rises from 0.59 to 0.62, and the maximum value increases from 0.82 to 0.89, a nearly 10% jump.

6.6 Equilibrium Campaign Effort

In equilibrium, candidates choose how to allocate campaign effort across battleground states to maximize their probability of winning the national election. The impact of effort on the utility differential is governed by the function

$$u(e_{s,p}) = \theta e_{s,p}^{1/\gamma}.$$

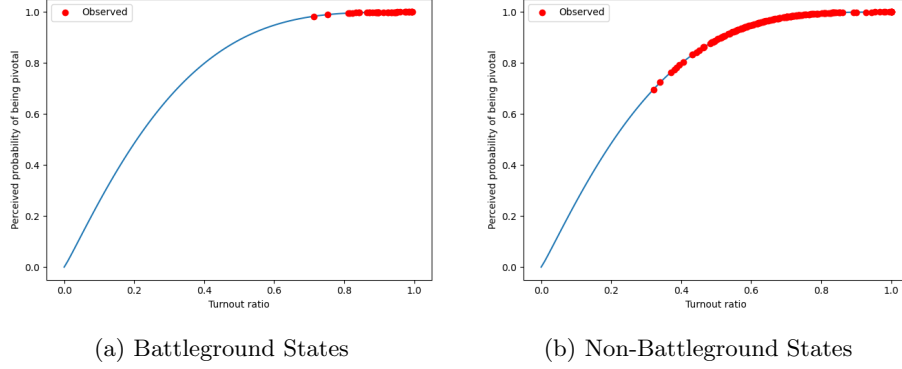


Figure 6: Estimated perceived probability of being pivotal as a function of the turnout ratio. Blue lines plot (??) evaluated at $(\hat{\alpha}_1, \hat{\alpha}_2) = (1.07, 3.41)$. Red circles are county-year observations.

A grid search over values of γ yields $\gamma = 3.0$, while the maximum likelihood estimate for θ is $\hat{\theta} = 0.044$. This corresponds to an average utility gain of approximately 0.03 across battleground states and election years. This is a nontrivial shift, given that the median baseline partisan utility difference $|\mu_{j_s}|$ is around 0.22.

To quantify marginal responsiveness, I exploit the equilibrium conditions for county-level turnout, defined in equations (1) and (2). In equilibrium, the following system must be satisfied for each county j_s in state s and each party $p \in \{D, R\}$:

$$\sigma_{s,p} = \sum_{j_s \in J_s} w_{j_s} \sigma_{j_s,p}, \quad p(\sigma_s) := p(\sigma_{s,D}, \sigma_{s,R}).$$

$$F_{j_s,D}(\mathbf{e}, \boldsymbol{\sigma}) = \sigma_{j_s,D} - H\left(u(e_{s,D}) - \mu_{j_s} - \frac{c_{j_s}}{p(\sigma_s)} + \eta_{j_s} + \delta_s - \eta_{j_s}^p\right) = 0, \quad (16)$$

$$F_{j_s,R}(\mathbf{e}, \boldsymbol{\sigma}) = \sigma_{j_s,R} - H\left(u(e_{s,R}) + \mu_{j_s} - \frac{c_{j_s}}{p(\sigma_s)} - \eta_{j_s} - \delta_s - \eta_{j_s}^p\right) = 0, \quad (17)$$

Stacking equations (16) and (17) over all counties in a given state yields the vector-valued function $F(\mathbf{e}, \boldsymbol{\sigma}) \in \mathbf{R}^{2|J|}$. The Jacobians $\partial F / \partial \boldsymbol{\sigma}$ and $\partial F / \partial \mathbf{e}$ enter the implicit function theorem:

$$\frac{\partial \boldsymbol{\sigma}}{\partial \mathbf{e}} = - \left(\frac{\partial F}{\partial \boldsymbol{\sigma}} \right)^{-1} \left(\frac{\partial F}{\partial \mathbf{e}} \right),$$

which is used to compute marginal turnout responses to changes in campaign effort.

From these derivatives, I compute county-level elasticities of the form

$$\varepsilon_{j_s,p,q} = \left(\frac{\partial \sigma_{j_s,p}}{\partial e_{s,q}} \right) \left(\frac{e_{s,q}}{\sigma_{j_s,p}} \right), \quad p, q \in \{D, R\},$$

Table 16 reports the average elasticity for each (p, q) pair across all battleground states and election years, weighted by the county population.

Table 16: Mean elasticity of turnout with respect to own and opponent effort

	Effort (D)	Effort (R)
Turnout _D	0.030	0.000
Turnout _R	0.000	0.023

A 1% increase in Democratic effort raises Democratic turnout by roughly 0.03%, with no measurable impact on Republican turnout; the reverse holds symmetrically. These modest own-elasticities suggest that campaigns operate in a region of diminishing returns, where additional effort yields increasingly smaller turnout gains, while the near-zero cross-elasticities suggest that changes in one party’s effort have little effect on the competitiveness of the race. Since the pivotality function $p(\cdot)$ remains largely unchanged, there is limited indirect influence on the opposing party’s turnout.

As discussed in Section 7, campaign effort still exerts a meaningful influence on average voter behavior. However, at current spending levels, the marginal voter is far less responsive.

6.7 Model Fit and Validation

The model’s credibility hinges on whether the equilibrium effort vector resembles how campaigns actually deploy resources across swing states. Because no single data set covers every outreach channel, I compile four proxies for the 2008–2020 cycles: (i) television-advertising dollars from the Wesleyan Media Project, (ii) in-person presidential and vice-presidential visits, (iii) Facebook ads in 2020 from OpenSecrets, and (iv) the state-level Romney ground-game index for 2012 constructed by Enos and Fowler (2018). In the following, I convert raw totals to state shares. For instance, in 2008 the Democratic candidate conducted 50 presidential visits. 12 of these were to Florida, meaning 24% of the total presidential visits by the Democratic candidate were allocated to Florida.

Table 17 reports two diagnostics of model fit: the Pearson correlation between predicted and observed state-level effort shares, and the root-mean-squared error (RMSE, in percentage points). Digital advertising aligns most closely with the model’s predicted allocations, particularly for Democrats (correlation $\rho = 0.934$, RMSE = 4.90), with a slightly weaker fit for Republicans ($\rho = 0.793$, RMSE = 6.70). Television ads also show strong correspondence (Democrats: $\rho = 0.748$, RMSE = 4.80; Republicans: $\rho = 0.706$, RMSE = 5.10). In-person

proxies perform less well: for presidential visits, correlations fall to $\rho = 0.639$ for Democrats and $\rho = 0.573$ for Republicans, with RMSEs around 6 percentage points. The Romney ground game index, available for Republicans in 2012, shows a correlation of $\rho = 0.729$ and $\text{RMSE} = 4.50$.

These patterns are consistent with the assumptions embedded in the effort technology $u(e) = \theta e^{1/\gamma}$, which treats effort as perfectly divisible and uniformly distributed across a state. Digital ads, which are highly granular, conform closely to this structure. Television buys fit less well, likely because they are purchased by media market rather than state boundary, introducing geographic mismatch. The poorest fit arises for candidate visits, which are both lumpy and subject to scheduling frictions, making them difficult to reconcile with the model’s continuous-effort framework.

Table 17: Fit statistics by effort proxy and party

Effort proxy	Correlation ρ		RMSE	
	Dem	Rep	Dem	Rep
Television ads (Wesleyan)	0.748	0.706	4.80	5.10
Presidential candidate visits	0.639	0.573	6.60	6.00
Digital ads (2020 only)	0.934	0.793	4.90	6.70
Romney ground game (2012 only)	–	0.729	–	4.50

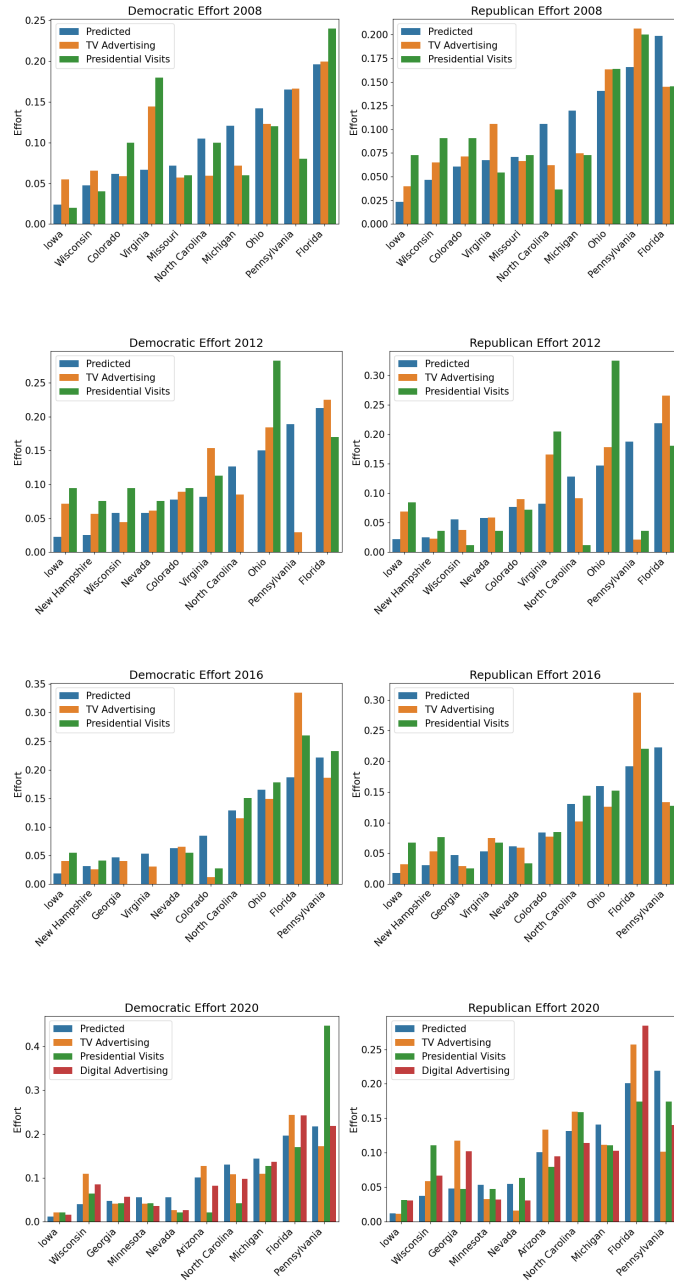
Correlation and RMSE values reflect the match between predicted effort shares and observed proxies by state. RMSE is computed as $\sqrt{\frac{1}{S} \sum_s (\hat{e}_s - e_s)^2}$ and reported in percentage points of total national share. The Romney index is available for the Republican campaign only; digital ad data is limited to 2020.

Figure 7 visualises the match by year. Within each panel, states are ordered by predicted effort (blue bars). Orange bars show the share of television advertising dollars allocated to each state, and green bars show the share of in-person visits. For 2020, I also include Facebook ad shares (red bars). The tallest bars such as Florida line up closely, while low-priority states such as Iowa stay at the bottom. This alignment provides strong validation for the model’s predictions.

7 Discussion

This section examines two implications for voter turnout and campaign behavior. First, I decompose the respective contributions of electoral competitiveness, captured through perceived voting efficacy, and direct campaign mobilization. Second, I address the puzzle of why campaigns invest heavily in mobilization despite modest experimental treatment effects, showing how the model reconciles low marginal returns with relatively low average costs per vote.

Figure 7: Estimated Effort Levels by Election Year



7.1 Disentangling Competition and Effort

This subsection uses the model to disentangle the effects of electoral competitiveness and direct campaign mobilization on voter turnout. I conduct a series of counterfactual simulations that remove or add these components in turn, holding fixed all other model elements, in order to isolate their marginal influence on turnout levels.

Battleground States. I begin from the observed equilibrium in battleground states and conduct a two-step counterfactual. First, I eliminate campaign mobilization by setting $e_{s,D} = e_{s,R} = 0$ in equations (1) and (2), holding fixed the state’s equilibrium level of voting efficacy. Second, I lower competitiveness by replacing p_s with the average value observed in non-battleground states, $p_s = 0.95$.

As reported in Table 18, the equilibrium turnout rate in battleground states is 62.6%. Removing effort alone reduces turnout to 58.2%, and further lowering voting efficacy brings turnout to 56.2%. This decomposition attributes approximately 70% of the total decline to the absence of campaign mobilization and 30% to reduced competitiveness.

The same pattern holds when measuring turnout in absolute terms. Eliminating effort reduces turnout by 2.9 million votes across battleground states, and lowering efficacy adds an additional loss of 1.3 million votes, resulting in a combined decline of 4.2 million. Consistent with the rate-based decomposition, approximately 70% of the decline is attributable to the removal of campaign effort, and the remaining 30% to reduced electoral competitiveness.

Non-Battleground States. A reverse counterfactual applied to non-battleground states evaluates how turnout would respond if these states were endowed with the characteristics of battleground states. These states start from an average equilibrium turnout of 56.5%, reflecting low pivotality and minimal campaign effort (see Table 18). First, I replace the pivotality p_s with the average value observed in battleground states, $p_s = .99$, while continuing to hold campaign effort at zero. This adjustment increases turnout to 58.5%, a gain of 2.0 percentage points. Introducing campaign effort comparable to that observed in battlegrounds yields a further 4.1-point increase, bringing turnout to 62.6%—identical to the equilibrium level in swing states. In this decomposition, enhanced competitiveness accounts for roughly one-third of the total turnout gain, while campaign effort contributes the remaining two-thirds.

A similar pattern emerges when turnout is measured in absolute terms. Raising pivotality alone, while holding campaign effort at zero, generates an additional 2.6 million votes relative to the baseline. Introducing battleground-level campaign effort adds a further 6.8 million votes, resulting in a total increase of 9.4 million ballots cast. These results mirror those based on turnout rates: approximately 73% of the gain is attributable to campaign effort, with the remaining 27% due to increased competitiveness.

Summary. Direct campaign effort clearly stands as the more dominant influence in shaping turnout differences between battleground and non-battleground environments, accounting for approximately 70% of the explained variation. Yet, the role of electoral competition and its effect on perceived pivotality is also fundamentally important, driving a substantial 30% of the counterfactual turnout changes. This dual significance underscores a key takeaway: while campaign mobilization exerts the stronger pull, the underlying competitiveness of an election remains an independently critical factor, and both elements must be central to any comprehensive understanding of voter turnout.

Table 18: Counterfactual Turnout Decomposition

Voting Efficacy	Effort	Turnout	Diff.	Share	Votes
<i>Battleground States</i>					
Equilibrium	Equilibrium	0.626	—	—	40.90M
Equilibrium	Zero	0.582	-0.044	0.696	38.00M
Avg. efficacy of non-BG states	Zero	0.562	-0.019	0.304	36.68M
<i>Non-Battleground States</i>					
Equilibrium	Zero	0.565	—	—	92.59M
Avg. efficacy of BG states	Zero	0.585	0.020	0.329	95.16M
Avg. efficacy of BG states	Avg. BG	0.626	0.061	0.671	101.96M

Note: Turnout is the share of eligible voters. Votes are in millions. Differences are relative to the previous row within each panel. “Share” denotes the fraction of the total difference explained by that row’s component.

7.2 The Cost of Mobilising a Vote

Field experiments typically find modest turnout effects from campaign outreach (e.g., Aggarwal et al. (2023), Spenkuch and Toniatti (2018), and Gerber, Gimpel, et al. (2011)), yet presidential campaigns continue to invest hundreds of millions of dollars targeting battleground states. This pattern reflects a disconnect between experimental findings and actual campaign behavior. The model reconciles this tension by distinguishing between marginal and average returns: although marginal effects are small at observed spending levels, the average cost per vote remains low enough to justify large-scale mobilization.

Let $V_{s,p}(e_{s,D}, e_{s,R})$ denote the model-implied vote total for party p in state s given efforts $e_{s,D}$ and $e_{s,R}$. The total effect of campaign effort on turnout is given by the difference in vote totals when moving from zero effort to equilibrium effort:

$$\Delta V_{s,p}^* = V_{s,p}(e_{s,D}^*, e_{s,R}^*) - V_{s,p}(0, 0).$$

where $e_{s,p}^*$ is the equilibrium effort level for party p in state s . This quantity captures the total number of votes gained by party p in state s due to campaign mobilization. The effect across the entire set of battleground states is given is

the sum of these differences:

$$\Delta V_p^* = \sum_{s \in BG} \Delta V_{s,p}^*,$$

where BG is the set of battleground states. Table 19 reports the estimated number of votes added by campaign mobilization in each presidential election cycle from 2008 to 2020, along with the corresponding turnout increases expressed in percentage points.

Table 19: Votes Added and Turnout Increase from Campaign Mobilization

Year	Votes Added			Turnout Increase (Percentage Points)		
	Dem	Rep	Total	Dem	Rep	Total
2008	1,612,266	1,293,502	2,905,768	2.40	1.93	4.33
2012	1,601,206	1,334,774	2,935,979	2.64	2.20	4.84
2016	1,212,333	1,238,404	2,450,738	1.82	1.86	3.69
2020	1,850,735	1,873,821	3,724,556	2.65	2.68	5.32

Note: “Votes Added” reports the estimated number of additional votes due to campaign mobilization, relative to a zero-effort counterfactual. “Turnout Increase” expresses the effect as an absolute change in turnout rate, in percentage points, using the voting-age population in battleground states as the denominator.

Taken together, these results show that campaign mobilization has a substantial effect on turnout in presidential elections. Across the four cycles, equilibrium effort generates between 2.4 and 3.7 million additional votes in battleground states. This translates to turnout increases of 3.7 to 5.3 percentage points, with similar gains for both parties. I now turn to the cost side of the mobilization calculus, distinguishing between the average and marginal cost per vote.

Average Cost per Vote (ACV). The average cost per vote within a given state, denoted $ACV_{s,p}$, is defined as

$$\bar{C}_{s,p} = \frac{e_{s,p}^*}{\Delta V_{s,p}^*}.$$

It reflects the average amount of effort required to generate one additional vote for party p in state s , relative to a no-effort baseline. This provides a measure of the overall cost-effectiveness of campaign mobilization at equilibrium effort levels.

Marginal Cost per Vote (MCV). The marginal cost of a vote for party p in state s , denoted $MCV_{s,p}$, measures how much additional campaign effort is

required to generate one more vote in that state. Formally, it is defined as the derivative of effort with respect to votes:

$$MCV_{s,p} = \frac{\partial e_{s,p}}{\partial V_{s,p}} = \left(\frac{\partial V_{s,p}}{\partial e_{s,p}} \right)^{-1}.$$

The total number of votes received by party p in state s is

$$V_{s,p} = \sum_{j_s \in s} \text{VAP}_{j_s} \cdot \sigma_{j_s,p},$$

where VAP_{j_s} is the voting-age population in county j_s , and $\sigma_{j_s,p}$ is the share of eligible voters in that county voting for party p . Differentiating with respect to campaign effort $e_{s,p}$ gives:

$$\frac{\partial V_{s,p}}{\partial e_{s,p}} = \sum_{j_s \in s} \text{VAP}_{j_s} \cdot \frac{\partial \sigma_{j_s,p}}{\partial e_{s,p}},$$

and taking the inverse yields the marginal cost of a vote:

$$MCV_{s,p} = \left(\sum_{j_s \in s} \text{VAP}_{j_s} \cdot \frac{\partial \sigma_{j_s,p}}{\partial e_{s,p}} \right)^{-1}.$$

Average and Marginal Costs per Vote in Equilibrium. I focus on both average and marginal costs per vote at the observed equilibrium effort levels, and examine how these costs vary with campaign scale. To do this, I scale the total available campaign effort ($E_{s,p}$) for each party in each state by a factor ϕ , where $\phi = 1.00$ corresponds to the observed equilibrium level. For each ϕ , I solve for the equilibrium of the model to obtain the optimal allocation of effort across states. I then recompute the average and marginal costs per vote using the simulated vote totals under the new allocation.

Table 20 reports average and marginal costs per vote under each counterfactual. At the observed (equilibrium) budget ($\phi = 1.00$), the average cost is modest: \$43.31 for Democrats, \$34.42 for Republicans. In contrast, the marginal cost at this level exceeds \$500, reflecting steep diminishing returns: as effort increases, campaigns must target progressively harder-to-mobilize voters, causing marginal cost to rise sharply.

Table 20: Average and Marginal Cost per Vote, by Effort Scale and Party

Effort Scale	Effort (\$M)		Avg. Cost (\$)		Marg. Cost (\$)	
	D	R	D	R	D	R
0.010	2.88	2.38	0.54	0.42	31.32	28.58
0.050	14.39	11.88	2.58	2.02	90.82	82.87
0.100	28.77	23.77	5.02	3.93	143.43	130.85
0.250	71.93	59.42	11.97	9.41	261.88	238.87
0.500	143.85	118.85	22.87	18.08	412.17	375.86
0.750	215.78	178.27	33.27	26.38	536.92	489.53
1.000	287.70	237.69	43.32	34.43	647.41	590.18
1.100	316.47	261.46	47.26	37.59	688.75	627.84
1.250	359.63	297.12	53.09	42.28	748.33	682.10
1.500	431.56	356.54	62.64	49.97	842.20	767.57

Note: Each row corresponds to a new equilibrium with rescaled total effort. Effort is reported in millions of dollars per party, averaged across battleground states and election years. Marginal cost is calculated at the new equilibrium.

The model thus reconciles a key puzzle: while field experiments often estimate small marginal effects of campaign outreach, these occur in contexts where most easy-to-mobilize voters have already been reached. From a campaign’s perspective, average cost is substantially lower.

Comparison to Experimental Estimates. To contextualize these findings, I compare the model’s predictions for marginal cost per vote to existing experimental estimates. I focus on two well-known studies that isolate the causal effect of (i) television advertising (Spenkuch and Toniatti 2018) and (ii) digital ads (Aggarwal et al. 2023). In each case I construct a counterfactual similar to the original experiment, but using the model’s equilibrium framework. This allows me to directly compare the model’s predictions to the experimental findings.

In Spenkuch and Toniatti (2018), the authors estimate the effect of television advertising on voter turnout by comparing turnout in counties on the border of advertising markets to those just outside the market. They find that television advertising has essentially no effect on turnout, but does meaningfully increase the vote share of the party running more ads.

In the model, I replicate this by removing the fraction of effort allocated to television advertising in battleground states, while leaving all other components unchanged. For instance, in the 2020 election, I find Republicans spent 47% of their campaign budget on television ads. I therefore multiply the equilibrium effort by 0.53 to simulate the effect of removing television ads. As the authors compare counties within the same state, I keep the competitiveness parameter p_s constant at the state’s equilibrium value.

Aggarwal and coauthors conduct a large-scale field experiment during the 2020 presidential election, randomly assigning \$8.9 million in digital advertise-

ments to two million moderate and low-information voters across five battleground states. This corresponds to an average treatment intensity of roughly \$4.5 per voter. To replicate this intervention within my state-level framework, I increase the Democratic effort in each of the five states by \$4.5 per voting-age resident, holding Republican effort fixed.

In both cases I compare the model’s predictions under the new equilibrium to the baseline equilibrium, which reflects the full campaign effort in each state.

Table 21: Turnout Effects: Model vs. Experimental Estimates

Experiment	Model Prediction			Experimental Estimate
	Total	Dem	Rep	
TV Ads Removed ^a	1.30	0.70	0.60	≈ 0.000
Digital Ads Added ^b	0.00	0.00	0.00	≈ 0.000

Note: Simulated turnout effects from field-experimental interventions. Results from model are average turnout across all counties in battleground states.

^a Spenkuch and Toniatti (2018) find no turnout effect from removing TV ads. The model removes TV effort in each battleground state.

^b Aggarwal et al. (2023) find no average turnout effect from a \$9 million digital ad campaign. The model adds \$4.5 per capita to Democratic digital effort across the battleground states

The model aligns with the null result in Aggarwal et al. (2023), predicting zero turnout effect from a modest increase in digital effort. Because the model treats effort as a composite input, this intervention captures the marginal return to campaign activity broadly—not to digital outreach specifically. In reality, an additional \$4.5 per capita in effort would be spent on the most cost-effective mobilization channels. Interpreting the treatment as digital-only likely overstates its potential impact, and the model-based prediction should be viewed as an upper bound on the effect of digital ads.

In contrast, removing television ads generates a 1.3 percentage point decline in turnout. This is substantially larger than the experimental null in Spenkuch and Toniatti (2018). This likely reflects a core limitation of the model: effort is a composite input, so removing the 47% associated with television reduces overall mobilization capacity without isolating a specific channel. The model assumes candidates reallocate effort optimally, cutting back first where marginal returns are lowest. As a result, the simulated demobilization is broader—and arguably more efficient—than in the experiment, which only alters television exposure while holding other outreach constant. The 1.3-point decline should be interpreted as an upper bound: in practice, losing half the campaign budget would constrain canvassing, digital, and other activities, not just television.

More broadly, the fact that turnout falls by only 1.3 percentage points when nearly half of campaign effort is removed implies that marginal mobilization costs are steep at observed effort levels. Most persuadable voters are already reached in equilibrium, so additional outreach yields sharply diminishing returns. This helps explain why field experiments often find limited effects:

marginal voters are inherently difficult to mobilize. Yet because the average cost per vote remains modest, large-scale mobilization remains cost-effective from the campaign’s perspective.

8 Conclusion

This paper develops and estimates a structural model of voter turnout that endogenises both electoral competitiveness and campaign mobilisation. By allowing presidential candidates to allocate finite resources across battleground states while anticipating county-level turnout responses, the framework unifies two literatures that are often studied in isolation. Maximum-likelihood estimation on county-level data from the 2008–2020 elections shows that differences in voting efficacy explain roughly fifteen percent of the turnout gap between battleground and non-battleground states, whereas direct mobilisation accounts for the remaining eighty-five percent. Although the marginal cost of generating an additional vote exceeds \$500 at observed spending levels, the average cost remains below \$45, which reconciles modest experimental treatment effects with the persistence of large campaign budgets.

The model also reproduces the geographic pattern of television and digital advertising, lending credibility to the inferred equilibrium strategies. At the same time, several simplifications warrant caution. First, the analysis treats safe states as receiving zero effort, which suppresses cross-state strategic spillovers. Second, while a grid search found that the optimal specification did not allow for cross-party persuasion, recent evidence suggests that persuasion can matter in some settings. Third, county-level shock variances are approximated away when computing the probability of winning a state; Monte Carlo exercises indicate that the approximation error is small, but it is not literally zero. Finally, the model is static and omits primary elections, donor dynamics, and sequential learning.

These limitations point to fertile directions for future research. Extending the framework to midterm or gubernatorial elections would test its robustness in contexts with lower salience and smaller electorates. Introducing cross-party persuasion, heterogeneous media markets, and dynamic budget accumulation could further sharpen the estimates of marginal returns. A richer treatment of election-law reforms, such as automatic voter registration or vote-by-mail expansions, would permit a more precise evaluation of policy counterfactuals. In addition, pairing the structural approach with high-frequency advertising data and micro-level experiments would improve identification of the effort-to-utility mapping.

Despite these caveats, the findings have immediate implications for both scholars and practitioners. Empirical work that seeks to infer the causes of turnout should account for the interaction between competitiveness and mobilisation rather than treating one channel as a nuisance. Campaign strategists should recognise that additional spending in highly saturated battlegrounds faces sharply diminishing returns, implying that the next frontier for cost-

effective mobilisation may lie in peripheral but competitive states. Election administrators and policymakers should understand that reforms lowering participation costs can magnify the turnout impact of campaign activity by raising voting efficacy, thereby amplifying representational equity.

Taken together, the paper clarifies why campaigns continue to invest heavily in voter outreach despite apparently small marginal effects and underscores the importance of modelling strategic behaviour on both sides of the electoral marketplace. By embedding voters and candidates in a common equilibrium, the approach provides a coherent foundation for analysing the incentives that underpin turnout, resource allocation, and ultimately electoral representation in the United States.

A Miscellaneous Tables and Figures

A.1 Accuracy of the county-shock approximation

This appendix quantifies the error that arises when county-level shocks η_{j_s} and $\eta_{j_s}^p$ are ignored in calculating the probability that the Democrat wins state s . I run $N_{\text{sim}} = 100$ Monte Carlo simulations. Each simulation contains $N_{\text{trial}} = 1,000$ independent shock draws used to estimate the relevant win probabilities.

Simulation design. In every simulation I proceed as follows:

1. Draw the number of precincts $n_s \sim \text{Unif}\{10, 100\}$.
2. Sample campaign efforts $e_{s,D}, e_{s,R} \sim \text{Unif}(0, 1)$.
3. Generate precinct-level heterogeneity μ_{j_s}, c_{j_s} , and weights w_{j_s} .
4. Draw pivotality-function parameters $\alpha_1 \in [0.5, 1.5]$ and $\alpha_2 \in [2, 5]$.
5. Draw utility parameters $\theta \sim \text{Unif}(0.1, 1)$ and $\gamma \sim \text{Unif}(2, 8)$.
6. Sample shock standard deviations $\sigma_\eta \in [0.10, 0.25]$ and $\sigma_\delta \in [0.25, 1.00]$.

These values are chosen to ensure that the model is well-behaved, and are of similar magnitude to the parameter values found in the maximum likelihood estimation in the main text.

I then draw N_{trial} independent realizations of the shocks:

$$\eta_{j_s} \sim \mathcal{N}(0, \sigma_\eta^2), \quad \eta_{j_s}^p \sim \mathcal{N}(0, \sigma_\eta^2), \quad \delta_s \sim \mathcal{N}(0, \sigma_\delta^2),$$

and estimate the two probabilities:

$$\begin{aligned} P_D^{\text{full}} &= \Pr[\sigma_{s,D}(\eta, \eta^p, \delta) > \sigma_{s,R}(\eta, \eta^p, \delta)], \\ P_D^{\text{approx}} &= \Pr[\sigma_{s,D}(0, 0, \delta) > \sigma_{s,R}(0, 0, \delta)], \end{aligned}$$

by computing the fraction of trials where the Democrat wins. $\sigma_{s,D}(\eta, \eta^p, \delta)$ and $\sigma_{s,R}(\eta, \eta^p, \delta)$ are the equilibrium strategies defined in 1 and 2, respectively, with the shocks η_{j_s} and $\eta_{j_s}^p$ set to zero for the approximation.

Results. Across the N_{sim} the Mean Squared Error (MSE), calculated as

$$\text{MSE} = \frac{1}{N_{\text{sim}}} \sum_{i=1}^{N_{\text{sim}}} (P_{D,i}^{\text{full}} - P_{D,i}^{\text{approx}})^2$$

is 0.00021. Several simulations yeild a difference of exactly 0.0.

A.2 Numerical verification of the uniqueness of $\hat{\delta}_s$

This section validates that the threshold value $\hat{\delta}_s$ defined in 6 is unique for a broad range of parameter values and campaign-effort profiles.¹⁵

Simulation design. For each replication, I:

1. Draw the number of precincts $n_s \sim \text{Unif}\{10, 100\}$.
2. Sample effort levels $e_{s,D}, e_{s,R} \sim \text{Unif}(0, 1)$.
3. Generate heterogeneity in baseline partisanship μ_{j_s} and voting costs c_{j_s} .
4. Assign precinct weights w_{j_s} and voting-eligible population shares.
5. Draw the two shape parameters of the perceived pivotality function

$$p(\sigma_{s,D}, \sigma_{s,R}) = 1 - (1 - \sigma_s^{\alpha_1})^{\alpha_2},$$

with $\alpha_1 \in [0.5, 1.5]$ and $\alpha_2 \in [2, 5]$.

6. Draw $\theta \sim \text{Unif}(0.1, 1)$ and $\gamma \sim \text{Unif}(2.0, 8.0)$.

These values are chosen to ensure that the model is well-behaved, and are of similar magnitude to the parameter values found in the maximum likelihood estimation in the main text.

For each of the $N_{\text{sim}} = 1,000$ Monte Carlo simulations, I attempt to solve for $(\hat{\delta}_s, \sigma_{s,D}, \sigma_{s,R})$ from 6, using $N_{\text{trial}} = 100$ *independent* random initial guesses. The root-finding routine is a damped Newton method implemented in **JAX**; the Jacobian is computed via automatic differentiation.

Outcome metric. Let $\delta^{(r,t)} = (\hat{\delta}_s, \sigma_{s,D}, \sigma_{s,R})^{(r,t)}$ denote the solution in simulation r (out of N_{sim}) and trial t (out of N_{trial}). Trials that do not yield a fixed point are discarded, as are trials that converge to the degenerate boundary solution $(x, 0, 0)$.

To assess the dispersion of solutions across trials, I compute the coordinate-wise variance

$$\text{Var}_t(\delta^{(r,t)}) = (\text{Var}_t(\hat{\delta}_s^{(r,t)}), \text{Var}_t(\sigma_{s,D}^{(r,t)}), \text{Var}_t(\sigma_{s,R}^{(r,t)})),$$

where $\text{Var}_t(\cdot)$ denotes variance across trials t within a given simulation r . If multiple distinct roots existed, at least one coordinate of this vector would be strictly positive.

Results. Across the 1,000 simulations, the largest coordinate-wise variance observed is given in Table 23.

¹⁵For some parameter combinations, two distinct fixed points may exist: an interior solution and a degenerate boundary solution of the form $(x, 0, 0)$, where x satisfies 6 under $\sigma_{s,D} = \sigma_{s,R} = 0$. I exclude this degenerate case from the analysis as it does not correspond to a meaningful equilibrium.

As evidence by the results, in every simulation, one of the following occurred: (a) the initial guess converged to a unique interior fixed point; (b) the Newton iterates diverged to the boundary $(x, 0, 0)$ and were excluded; or (c) the solver failed to converge. Given that a valid interior solution is found in every parameter draw and the observed variance is vanishingly small, I conclude that the solution to 6 is *globally unique* for any feasible parameter configuration. Hence, the smoothed probability of winning a state, $\tilde{p}_s(e_{s,D}, e_{s,R}) = 1 - F(\hat{\delta}_s)$, is well-defined.

B Constructing Campaign Budget Shares and Total Effort

B.1 Data Sources

Campaign-finance information comes from two datasets:

- *Television advertising.* Gross state-level outlays on presidential television ads are provided by the Wesleyan Media Project. These figures form the variable $TV_{s,p}$ discussed in Section ??.
- *Operating expenditures.* Itemised operating-expenditure files released by the Federal Election Commission (FEC) record every payment made by candidate committees, including transaction date, amount, and free-text purpose description.

B.2 Filtering Operating Expenditures

The raw FEC files contain many transactions unrelated to voter mobilisation. The following rules are applied to retain only plausible mobilisation outlays:

1. **General-election focus:** Keep entries tagged as general or general-primary spending.
2. **Candidate committees:** Restrict to disbursements by the principal presidential committees of each major party.
3. **Purpose description cleaning:** Convert purpose strings to lower-case and harmonise common variants (e.g. “on-line” \rightarrow “online”).
4. **Positive keyword match:** Retain only transactions whose purpose description matches one of the five predefined mobilization categories (media, online, print, telemarketing, travel) based on regular expressions.

B.3 Classifying Mobilisation Channels

Every retained transaction is assigned to one of five mutually exclusive mobilisation categories using keyword patterns:

Category	Matched keywords in purpose description
media	media, tv, broadcast
online	online, digital, facebook, google, youtube, twitter, instagram, snapchat, web, internet
print	print, post, mail, leaflet
telemarketing	telemarketing, phone, text, sms
travel	travel, event, rally, airfare, hotel

Ambiguous strings are resolved by a priority order $\text{media} \succ \text{online} \succ \text{print} \succ \text{telemarketing} \succ \text{travel}$, ensuring each transaction appears exactly once.

B.4 National Category Shares

Let $\text{FEC}_{s,p,c}$ denote the sum of filtered disbursements made by party $p \in \{D, R\}$ in state s and category c during election cycle t . National spending shares are

$$\phi_{t,c} = \frac{\sum_{s,p} \text{FEC}_{s,p,c}}{\sum_{s,p,c} \text{FEC}_{s,p,c}}.$$

Because vendor locations are not reported, these shares are computed at the national (not state) level.

B.5 Normalising Relative to Television

Television is the only channel measured directly at the state level. To express the remaining categories in comparable units, I scale them by the ratio of national spending in category c to national spending on media:

$$\tilde{\phi}_{t,c}^p = \frac{\phi_{t,c}^p}{\phi_{t,\text{media}}^p}, \quad c \neq \text{media}.$$

B.6 Calculating Total Effort

For party p in swing state s and year t , total inferred mobilisation effort is

$$B_{s,p} = \text{TV}_{s,p} \left[1 + \sum_{c \neq \text{media}} \tilde{\phi}_{t,c}^p \right].$$

Aggregating over the swing-state set S_t yields the national swing-state totals reported in Table 12:

$$\text{Effort}_{p,t} = \sum_{s \in S_t} B_{s,p}.$$

Replication materials, including cleaned expenditure files and code to recreate all tables, are available upon request or via the project’s online repository.

References

- Aggarwal, Minali et al. (2023). “A 2 million-person, campaign-wide field experiment shows how digital advertising affects voter turnout”. In: *Nature Human Behaviour* 7.3, pp. 332–341.
- Ainsworth, Robert, Emanuel Garcia Munoz, and Andres Munoz Gomez (2022). “District competitiveness increases voter turnout: evidence from repeated redistricting in North Carolina”. In: *University of Florida*.
- Ashworth, Scott, Joshua D Clinton, et al. (2007). “Does advertising exposure affect turnout?” In: *Quarterly Journal of Political Science* 2.1, pp. 27–41.
- Bagwe, Gaurav, Juan Margitic, and Allison Stashko (2022). *Polling Place Location and the Costs of Voting*. Tech. rep. Technical Report. https://jmargitic.github.io/JM/Margitic_JMP.pdf.
- Bonica, Adam et al. (2021). “All-mail voting in Colorado increases turnout and reduces turnout inequality”. In: *Electoral studies* 72, p. 102363.
- Burden, Barry C et al. (2014). “Election laws, mobilization, and turnout: The unanticipated consequences of election reform”. In: *American Journal of Political Science* 58.1, pp. 95–109.
- Bursztyn, Leonardo et al. (2024). “Identifying the effect of election closeness on voter turnout: Evidence from swiss referenda”. In: *Journal of the European Economic Association* 22.2, pp. 876–914.
- Cantoni, Enrico (2020). “A precinct too far: Turnout and voting costs”. In: *American Economic Journal: Applied Economics* 12.1, pp. 61–85.
- Cantoni, Enrico and Vincent Pons (2021). “Strict ID laws don’t stop voters: Evidence from a US nationwide panel, 2008–2018”. In: *The Quarterly Journal of Economics* 136.4, pp. 2615–2660.
- Castanheira, Micael (2003). “Victory margins and the paradox of voting”. In: *European Journal of Political Economy* 19.4, pp. 817–841.
- Coate, Stephen and Michael Conlin (2004). “A group rule—utilitarian approach to voter turnout: Theory and evidence”. In: *American Economic Review* 94.5, pp. 1476–1504.
- Coate, Stephen, Michael Conlin, and Andrea Moro (2008). “The performance of pivotal-voter models in small-scale elections: Evidence from Texas liquor referenda”. In: *Journal of Public Economics* 92.3-4, pp. 582–596.
- Downs, Anthony (1957). “An economic theory of political action in a democracy”. In: *Journal of political economy* 65.2, pp. 135–150.
- Enos, Ryan D and Anthony Fowler (2018). “Aggregate effects of large-scale campaigns on voter turnout”. In: *Political Science Research and Methods* 6.4, pp. 733–751.
- Fraga, Bernard L, Daniel J Moskowitz, and Benjamin Schneer (2022). “Partisan alignment increases voter turnout: Evidence from redistricting”. In: *Political behavior* 44.4, pp. 1883–1910.
- Gerber, Alan S (2004). “Does campaign spending work? Field experiments provide evidence and suggest new theory”. In: *American Behavioral Scientist* 47.5, pp. 541–574.

- Gerber, Alan S, James G Gimpel, et al. (2011). “How large and long-lasting are the persuasive effects of televised campaign ads? Results from a randomized field experiment”. In: *American Political Science Review* 105.1, pp. 135–150.
- Gerber, Alan S and Donald P Green (2000). “The effects of canvassing, telephone calls, and direct mail on voter turnout: A field experiment”. In: *American political science review* 94.3, pp. 653–663.
- Gerber, Alan S, Gregory A Huber, and Seth J Hill (2013). “Identifying the effect of all-mail elections on turnout: Staggered reform in the evergreen state”. In: *Political Science research and methods* 1.1, pp. 91–116.
- Geys, Benny (2006). “Explaining voter turnout: A review of aggregate-level research”. In: *Electoral studies* 25.4, pp. 637–663.
- Grumbach, Jacob M and Charlotte Hill (2022). “Rock the registration: Same day registration increases turnout of young voters”. In: *The Journal of Politics* 84.1, pp. 405–417.
- Harden, Jeffrey J and Alejandra Campos (2023). “Who benefits from voter identification laws?” In: *Proceedings of the National Academy of Sciences* 120.7, e2217323120.
- Herrera, Helios, David K Levine, and Cesar Martinelli (2008). “Policy platforms, campaign spending and voter participation”. In: *Journal of Public Economics* 92.3-4, pp. 501–513.
- Kawai, Kei, Yuta Toyama, and Yasutora Watanabe (2021). “Voter turnout and preference aggregation”. In: *American Economic Journal: Microeconomics* 13.4, pp. 548–586.
- Li, Quan, Michael J Pomante, and Scot Schraufnagel (2018). “Cost of voting in the American states”. In: *Election Law Journal: Rules, Politics, and Policy* 17.3, pp. 234–247.
- Myatt, David P (2012). “A rational choice theory of voter turnout”. In: *London Business School*.
- Myerson, Roger B (2000). “Large poisson games”. In: *Journal of Economic Theory* 94.1, pp. 7–45.
- Nickerson, David W (2006). “Volunteer phone calls can increase turnout: Evidence from eight field experiments”. In: *American Politics Research* 34.3, pp. 271–292.
- Palfrey, Thomas R and Howard Rosenthal (1983). “A strategic calculus of voting”. In: *Public choice* 41.1, pp. 7–53.
- Riker, William H and Peter C Ordeshook (1968). “A Theory of the Calculus of Voting”. In: *American political science review* 62.1, pp. 25–42.
- Shachar, Ron and Barry Nalebuff (1999). “Follow the leader: Theory and evidence on political participation”. In: *American Economic Review* 89.3, pp. 525–547.
- Spenkuch, Jörg L and David Toniatti (2018). “Political advertising and election results”. In: *The Quarterly Journal of Economics* 133.4, pp. 1981–2036.
- Strömberg, David (2008). “How the Electoral College influences campaigns and policy: the probability of being Florida”. In: *American Economic Review* 98.3, pp. 769–807.

Thompson, Daniel M et al. (2020). “Universal vote-by-mail has no impact on partisan turnout or vote share”. In: *Proceedings of the National Academy of Sciences* 117.25, pp. 14052–14056.

Table 22: Estimated Coefficients for Partisan Bias Component (μ)

Parameter	Variable	Coefficient	Std. Error	P-Value
<i>Gender and Age</i>				
	Male (2008)	0.116	0.124	0.350
	Male (2012)	0.257	0.118	0.030
	Male (2016)	0.086	0.118	0.465
	Male (2020)	-0.221	0.114	0.052
	Age 18-29 (2008)	-0.353	0.073	0.000
	Age 18-29 (2012)	-0.545	0.076	0.000
	Age 18-29 (2016)	-0.668	0.079	0.000
	Age 18-29 (2020)	-0.765	0.078	0.000
	Age 65+ (2008)	-0.710	0.103	0.000
	Age 65+ (2012)	-0.971	0.101	0.000
	Age 65+ (2016)	-1.019	0.095	0.000
	Age 65+ (2020)	-1.223	0.089	0.000
<i>Race and Ethnicity</i>				
	White (2008)	1.252	0.218	0.000
	White (2012)	1.461	0.226	0.000
	White (2016)	1.089	0.215	0.000
	White (2020)	1.051	0.162	0.000
	Black (2008)	0.083	0.219	0.705
	Black (2012)	0.108	0.227	0.633
	Black (2016)	-0.376	0.216	0.081
	Black (2020)	-0.498	0.163	0.002
	Native American (2008)	0.326	0.235	0.166
	Native American (2012)	0.419	0.241	0.082
	Native American (2016)	0.007	0.226	0.975
	Native American (2020)	-0.219	0.169	0.197
	Asian (2008)	1.517	0.290	0.000
	Asian (2012)	1.718	0.297	0.000
	Asian (2016)	1.316	0.279	0.000
	Asian (2020)	1.502	0.223	0.000
	Hispanic (2008)	0.544	0.219	0.013
	Hispanic (2012)	0.579	0.225	0.010
	Hispanic (2016)	0.142	0.214	0.507
	Hispanic (2020)	0.121	0.160	0.450
<i>Education</i>				
	High School Only (2008)	-0.264	0.090	0.003
	High School Only (2012)	-0.492	0.097	0.000
	High School Only (2016)	-0.158	0.098	0.107
	High School Only (2020)	-0.244	0.096	0.011
	Some College (2008)	0.446	0.077	0.000
	Some College (2012)	0.248	0.083	0.003
	Some College (2016)	0.504	0.085	0.000
	Some College (2020)	0.310	0.085	0.000
	College Only (2008)	0.208	0.106	0.050
	College Only (2012)	0.142	0.106	0.178
	College Only (2016)	-0.191	0.106	0.071
	College Only (2020)	-0.469	0.100	0.000
	College+ (2008)	-1.767	0.150	0.000
	College+ (2012)	-1.749	0.149	0.000
	College+ (2016)	-1.938	0.144	0.000
	College+ (2020)	-2.126	0.129	0.000

Table 23: Dispersion of $(\hat{\delta}_s, \sigma_{s,D}, \sigma_{s,R})$ across random initialisations

	$\hat{\delta}_s$	$\sigma_{s,D}$	$\sigma_{s,R}$
$\max_r \text{Var}_t(\cdot)$	1.37×10^{-23}	5.05×10^{-22}	5.28×10^{-22}

Note: Values report the largest coordinate-wise variance observed over $N_{\text{sim}} = 1,000$ simulations and $N_{\text{trial}} = 100$ random starting points per simulation. The vanishing dispersion indicates convergence to a *single* fixed point in every replication.